Molecular Therapy
Original Article

PTB-AS, a Novel Natural Antisense Transcript, Promotes Glioma Progression by Improving PTBP1 mRNA Stability with SND1

Liyuan Zhu,[1,5] Qunfang Wei,[1,5] Yingjiao Qi,[1] Xiangbin Ruan,[1] Fan Wu,[1] Liang Li,[1] Junjie Zhou,[1] Wei Liu,[1] Tao Jiang,[3,4] Jing Zhang,[1] Bin Yin,[1] Jiangang Yuan,[1] Boqin Qiang,[1] Wei Han,[1,7] and Xiaozhong Peng[1,2,6]

[1]State Key Laboratory of Medical Molecular Biology, Department of Molecular Biology and Biochemistry, Institute of Basic Medical Sciences, Medical Primate Research Center, Neuroscience Center, Chinese Academy of Medical Sciences, School of Basic Medicine Peking Union Medical College, Beijing, China; [2]Institute of Medical Biology, Chinese Academy of Medical Sciences, Peking Union Medical College, Kunming, China; [3]Department of Neurosurgery, Beijing Tiantan Hospital, Capital Medical University, Beijing, China; [4]Department of Molecular Neuropathology, Beijing Neurosurgical Institute, Capital Medical University, Beijing China

Glioma, the most common primary malignancy in the brain, has high recurrence and lethality rates, and thus, elucidation of the molecular mechanisms of this incurable disease is urgently needed. Poly-pyrimidine tract binding protein (PTBP1, also known as hnRNP I), an RNA-binding protein, has various mechanisms to promote gliomagenesis. However, the mechanisms regulating PTBP1 expression are unclear. Herein, we report a novel natural antisense noncoding RNA, PTB-AS, whose expression correlated positively with PTBP1 mRNA. We found that PTB-AS significantly promoted the proliferation and migration *in vivo* and *in vitro* of glioma cells. PTB-AS substantially increased the PTBP1 level by directly binding to its 3′ UTR and stabilizing the mRNA. Furthermore, staphylococcal nuclease domain-containing 1 (SND1) dramatically increased the binding capacity between PTB-AS and PTBP1 mRNA. Mechanistically, PTB-AS could mask the binding site of miR-9 in the PTBP1-3′ UTR; miR-9 negatively regulates PTBP1. To summarize, we revealed that PTB-AS, which maintains the PTBP1 level through extended base pairing to the PTBP1 3′ UTR with the assistance of SND1, could significantly promote gliomagenesis.

INTRODUCTION

Glioma is the most common type of malignant primary brain tumor, with high recurrence and lethality rates.[1] The treatment and prognosis of severely ill patients with glioma have shown no significant improvements despite advances in surgery, radiation therapy, and chemotherapy.[2] Thus far, the mechanisms of gliomagenesis include the alternative expression of core genes (signal transducer and activator of transcription 3 [STAT3]; positively).[3] RNA-binding proteins (RBPs), which can bind to single- or double-stranded RNAs, also participate in regulating gliomagenesis.[4] RBPs, which are important and functional protein-coding genes, could influence pre-mRNA processing, as well as the transport, localization, translation, and stability of mRNAs.[5] Our research has focused on the regulation of RBPs in glioma, and we previously performed a systematic functional study of poly(RC) binding protein 2 (PCBP2) and adenosine deaminase RNA specific 1 (ADAR1).[6,7] which play important roles in gliomagenesis. In this study, we further explored the regulatory mechanism of another important RBP, poly-pyrimidine tract binding protein (PTBP1), which was dramatically overexpressed in glioma.

PTBP1, also known as hnRNP I, is an RBP with various molecular functions. Upregulating PTBP1 in differentiated cells contributes to gliomagenesis through aberrantly modulating the alternative splicing of genes involved in cell proliferation and migration, including fibroblast growth factor receptor-1 (FGFR-1), pyruvate kinase M (PKM), and ubiquitin-specific peptidase 5 (USP5).[8] In addition to its role in splicing, PTBP1 is involved in other aspects of mRNA metabolism, such as 3′ end processing, transport, stability, and internal ribosome entry site (IRES)-mediated translation.[9] Although PTBP1 has been extensively investigated, given its crucial role in neural development and gliomagenesis,[9] the mechanisms regulating its own expression have been poorly explored. Thus

Received 23 October 2018; accepted 29 May 2019;
https://doi.org/10.1016/j.ymthe.2019.05.023.

[5]These authors contributed equally to this work.

[6]Present address: Xiaozhong Peng, State Key Laboratory of Medical Molecular Biology, Institute of Basic Medical Sciences, Chinese Academy of Medical Sciences and Peking Union Medical College, Beijing 100005, China

[7]Present address: Wei Han, State Key Laboratory of Medical Molecular Biology, Institute of Basic Medical Sciences, Chinese Academy of Medical Sciences and Peking Union Medical College, Beijing 100005, China

Correspondence: Xiaozhong Peng, State Key Laboratory of Medical Molecular Biology, Department of Molecular Biology and Biochemistry, Institute of Basic Medical Sciences, Medical Primate Research Center, Neuroscience Center, Chinese Academy of Medical Sciences, School of Basic Medicine Peking Union Medical College, Beijing, China.
E-mail: pengxiaozhong@pumc.edu.cn
Correspondence: Wei Han, State Key Laboratory of Medical Molecular Biology, Department of Molecular Biology and Biochemistry, Institute of Basic Medical Sciences, Medical Primate Research Center, Neuroscience Center, Chinese Academy of Medical Sciences, School of Basic Medicine Peking Union Medical College, Beijing, China.
E-mail: hanwei2012@ibms.pumc.edu.cn

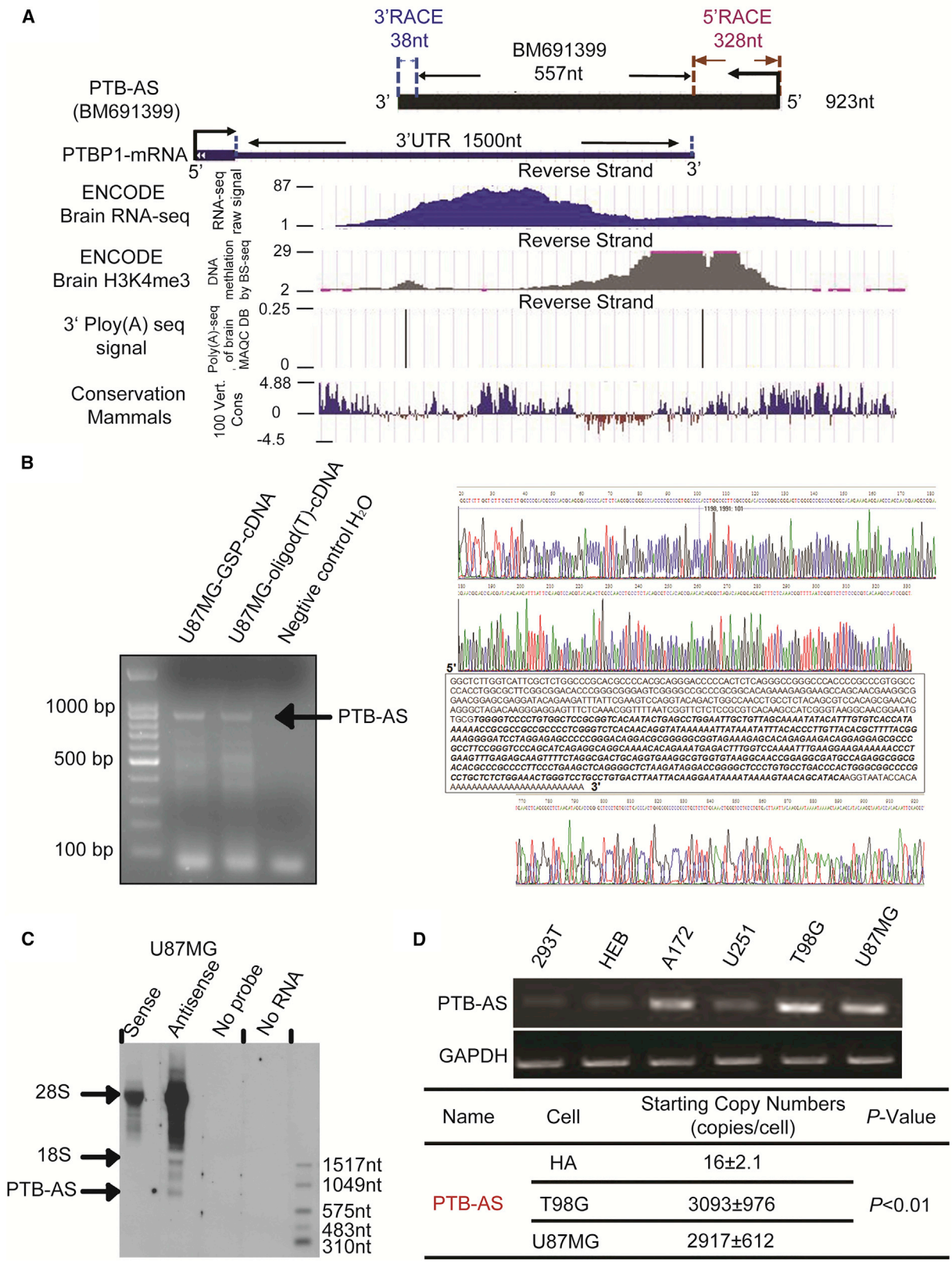

Name	Cell	Starting Copy Numbers (copies/cell)	*P*-Value
PTB-AS	HA	16±2.1	*P*<0.01
	T98G	3093±976	
	U87MG	2917±612	

(legend on next page)

far, the neuron-specific microRNA (miRNA) miR-124 has been shown to directly target PTBP1 mRNA and reduce PTBP1 protein levels, leading to the accumulation of correctly spliced PTBP2 mRNA and a dramatic increase in PTBP2 protein.[10] In addition, a previous reports showed that the transcription factor c-Myc directly controls the expression of hnRNPA1/A2 and PTBP1 and then regulates PKM alternative splicing in cancer.[11] However, whether long noncoding RNAs (lncRNAs) could influence PTBP1 expression is largely unknown.

Natural antisense transcripts (NATs) are a class of RNA molecules that are complementary to their paired RNA transcripts.[12] These molecules can be transcribed in *cis* from the opposing DNA strands at the same genomic locus or in *trans* at a separate genomic locus.[13] NATs may regulate sense-strand mRNAs in a positive (concordant) or negative (discordant) manner at the transcriptional or post-transcriptional level, to carry out a wide range of biological and cellular functions.[14,15] NATs have been found to function at several levels to regulate gene expression, including the pre-transcriptional, transcriptional, and post-transcriptional levels, through DNA-RNA, RNA-RNA, or protein-RNA interactions in the nucleus or cytoplasm.[16] The abnormal expression of NATs has been implicated in the pathogenesis of various diseases, such as cancer or neurological disease.[17] Furthermore, NATs were reported to have a close relationship with gliomagenesis. For example, HOXA11-AS was involved in cell cycle progression,[18] ZEB1-AS1 was an important regulator of migration and invasion via activating epithelial-to-mesenchymal transition (EMT) in the metastatic progression of glioma,[19] downregulation of HIF1A-AS2 led to delayed growth of mesenchymal glioblastoma (GBM) stem-like cell (GSC) tumors,[20] TP73-AS1 promotes brain glioma growth and invasion through acting as a competing endogenous RNA (ceRNA) to promote high mobility group box 1 (HMGB1) expression by sponging miR-142,[21] and PRKAG2-AS1 is indispensable for early diagnosis or prognosis of glioma.[22]

In the present study, we discovered that PTB-AS, a novel NAT transcribed from the reverse strand of the PTBP1 gene, partially overlaps with the 3′ UTR of the PTBP1 mRNA and plays an essential role in upregulating PTBP1 gene expression. Knockdown of PTB-AS significantly inhibited glioma proliferation (*in vitro* and *in vivo*) and migration. Mechanistically, PTB-AS directly bound to the 3′ UTR of PTBP1 mRNA, protect PTBP1 from being targeted by miR-9, and stabilize PTBP1-mRNA with the help of staphylococcal nuclease domain containing 1 (SND1). These findings elucidated a novel mechanism by which PTBP1 is upregulated in gliomagenesis and identified a novel NAT that could be a potential target for glioma therapy.

RESULTS

Identification of a Novel Antisense lncRNA, PTB-AS, at the PTBP1 Gene Locus

We searched an RBPs database and identified 380 putative RBPs (Table S1) spatially expressed in postmitotic or proliferating regions of the embryonic brain. To analyze the roles of NATs in glioma, we used the NATs Database (NATsDB) (http://natsdb.cbi.pku.edu.cn/)[12] to predict whether these RBPs have corresponding NATs in their genomic locus. We found that 199 RBPs (Table S2) had associated NATs (including 117 full overlapping NATs, 40 head-to-head NATs, and 42 tail-to-tail NATs), and 181 other RBPs were predicted to have no NATs in their genomic loci (Figure S1A). We screened the expression of genes among the 199 RBPs in glioma with the NCBI UniGene expressed sequence tab (EST) profile database and found that 23 genes were significantly highly expressed in glioma (data not shown). We found a NAT in the genomic locus of the PTBP1-3′ UTR (Figure S1B; Table S3); then, we identified it as a novel lncRNA and explored its function and mechanism.

The NAT of PTBP1, BM691399, is a transcript with a length of 557 nt that is completely located in the PTBP1-3′ UTR genomic locus. We analyzed the chromatin marks (H3K4me3) and RNA sequencing data (Encode RNA-seq signals and Poly(A)-seq] and identified the conservation quality among mammals. The results showed that the active transcription signal H3K4me3 exists upstream of BM691399 and that the whole genomic locus has RNA-seq signals in human brain tissue (Figure 1A). To verify the existence of this NAT, we detected its presence and relative abundance in glioma cells compared with normal cells. We identified a robust Poly(A) signal in the 3′ end of BM691399. To clone the full length of this NAT, we performed 5′ and 3′ rapid amplification of cDNA ends (RACE) and observed a distinct band near the 900 nt marker of 900 nt, regardless of the presence of 5′ gene-specific primer 1 (GSP1)-RT-cDNA or 3′ oligo(dT)-RT-cDNA template. We found that the full length of PTBP1 NAT was 923 nt after the strict sequencing step (Figures 1B and S1C). Northern blot analysis was employed to determine the full length of

Figure 1. Characterization of the Novel Antisense lncRNA PTB-AS at the PTBP1 Locus

(A) Genome-wide discovery of PTB-AS. PTB-AS (923 nt), derived from the transcript BM691399 (557 nt), was amplified by RACE and overlapped with the PTBP1-3′ UTR. RNA sequencing (RNA-seq) can directly define the transcribed regions of the genome, and the raw signal here shows the primary structure of PTB-AS. Chromatin marks of transcription initiation (histone H3 lysine 4 trimethylation [H3K4me3]) defined the beginning of PTB-AS, and sequencing of polyadenylation ends (3′ Poly(A)-seq) defined the precise ends of these transcripts. The 100 Vert. Cons scores describe the conservation of PTB-AS in mammals. All of these raw data were analyzed using the UCSC genome browser. (B) Identification of the full length of PTB-AS by strand-specific RT-PCR. The total RNA of U87MG cells was extracted. The first lane indicates products that used the GSP for RT as the template. The second lane indicates products that used the oligo (dT) primer for RT as the template. The third lane indicates products that used H_2O for RT as the template. The arrow shows the direction of the bands of PTB-AS. The raw sequencing spectrogram of RACE for PTB-AS is shown: the upper one is for 5′ RACE, and the lower one is for 3′ RACE. (C) Northern blot results indicate the full length of PTB-AS. An antisense probe hybridized with PTB-AS RNA, whereas the sense or no-probe and no-total RNA served as negative controls. The single band indicated by the arrow is PTB-AS. (D) Two normal human cell lines and four glioma cell lines were used to extract total RNA, which was reverse transcribed. Semiquantitative PCR was performed to identify the relative expression of the PTBP1 NAT. GAPDH served as the internal parameter reference. The copy number was detected and calculated to quantify the expression of PTB-AS in HA, T98G, or U87MG cell lines, using absolute qPCR.

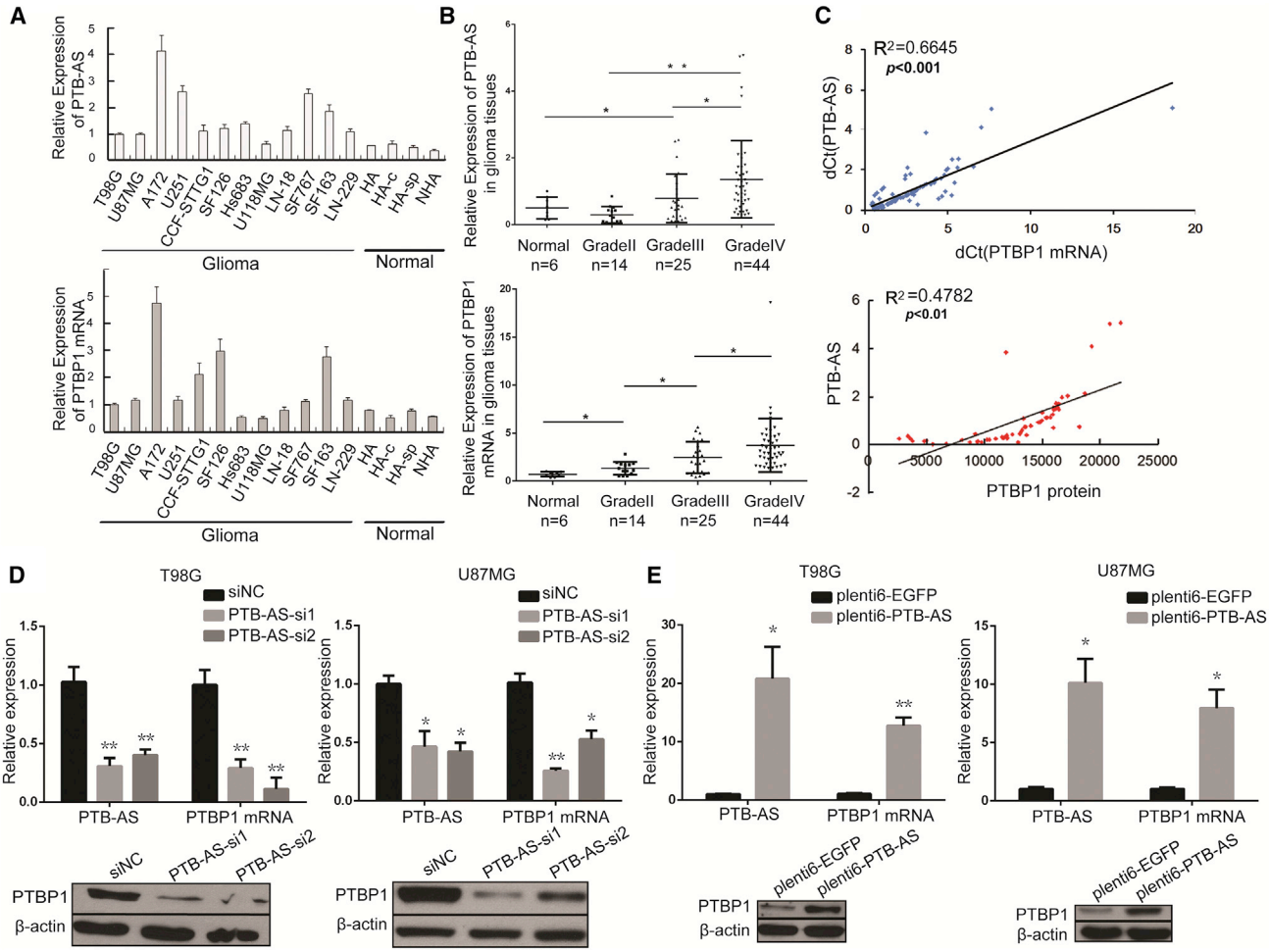

Figure 2. The Positive Correlation between PTB-AS and PTBP1 Expression and PTB-AS Regulates the PTBP1 mRNA and Protein Levels

(A and B) Expression of PTB-AS and PTBP1 mRNA in the (A) glioma cell lines (n = 12) compared to human normal astrocyte lines (n = 4) or (B) glioma tissues (n = 83) compared to normal brain tissues (n = 6) detected by quantitative real-time PCR. Expression data are presented as the mean ± SD, n = 3. *p < 0.05, **p < 0.01 (Student's t test). (C) Correlation analysis showing that PTB-AS correlated positively with PTBP1 mRNA or protein expression. The mRNA and protein expression levels were measured in the glioma tissue samples. The delta cycle threshold (dCt) values (normalized to GAPDH) were subjected to Pearson correlation analysis (Student's t test). (D and E) Changes in PTB-AS expression altered PTBP1 mRNA and protein levels. T98G cells and U87MG cells were infected with (D) two different siRNAs (PTB-AS si1 or PTB-AS si2) to knock down (siNC [small interfering negative control]) or (E) PTB-AS-plenti6 plasmid to overexpress PTB-AS (EGFP-plenti6 was the negative control). PTB-AS and PTBP1 mRNA expression were measured by quantitative real-time PCR. PTBP1 protein level was measured by western blot analysis, n = 3. *p < 0.05, **p < 0.01 (Student's t test).

this NAT, and we observed a distinct band near the 1,049 nt RNA marker only, in the probe hybridization treatment group (Figure 1C). Furthermore, the PTB-AS signal was weaker in the knockdown groups than the control group (Figure S1D). We named this NAT PTB-AS, because it originates from the complementary strand of the PTBP1 gene. We found that PTB-AS was upregulated in several glioma cell lines and the starting copy number of PTB-AS, or that PTBP1 was higher in glioma than in normal astrocyte cells (Figures 1D and S1E). To demonstrate the non-coding potential of PTB-AS, we used the classical prediction web server Coding Potential Calculator (CPC) and experimental identification. As a result, PTB-AS was found to be without coding capacity as a lncRNA (Figures S1F and S1G).

PTB-AS Is Upregulated in Glioma and Positively Regulates the PTBP1 Level

PTBP1 is overexpressed in glioma cell lines and tumor tissues and is essential for gliomagenesis.[2,23] To address the potential coregulation between PTB-AS and PTBP1, we primarily examined the expression of PTB-AS and PTBP1 mRNA. Our results showed that high expression of PTB-AS and PTBP1 mRNA was detected in 12 glioma cell lines compared with the normal astrocyte cell line (Figure 2A). Concordantly, PTB-AS and PTBP1 mRNA levels were upregulated in glioma tissue samples (n = 83) compared with control brain tissue samples (n = 6; Figure 2B). In addition, the PTBP1 protein level was significantly increased in the glioma cell lines and tissue samples (Figures S2A and S2B), which is consistent with the augmentation of

PTBP1 observed in glioma in previous studies.[24] To determine the potential relationship between PTB-AS expression and patient prognosis, we used the systematic database of the expression profiles and clinical data of genes or ncRNAs from the Chinese Glioma Genome Atlas (CGGA) database of Tiantan Hospital and the Oncomine and The Cancer Genome Atlas (TCGA) databases to screen our transcripts. Kaplan-Meier analysis and log-rank tests were used to evaluate the effects of PTB-AS and PTBP1 expression on overall survival (OS). The results indicated that patients with higher PTB-AS or PTBP1 expression had a significantly poorer prognosis than patients with lower expression ($p < 0.0001$; Figures S2C and S2D). PTB-AS and PTBP1 showed a similar expression pattern, suggesting that functionally related mechanisms may be present between these two transcripts.

Next, we used Pearson's correlation analysis to identify the relationship between PTB-AS and PTBP1 expression and found that PTB-AS was robustly positively correlated with PTBP1 mRNA, with statistical significance established at $p < 0.001$. PTB-AS transcripts also correlated positively with the PTBP1 protein ($p < 0.01$, Figure 2C). Given the close genomic proximity of PTB-AS and PTBP1, we hypothesized that PTB-AS could exert biological effects by modulating PTBP1. We used knockdown and overexpression analyses to test the influence of PTB-AS on PTBP1. The target sites of small interfering RNAs (siRNAs) were carefully chosen to avoid the overlap region with PTBP1 mRNA, as shown in Figure S3A. Quantitative real-time PCR and western blot analysis were performed to examine the effects of PTB-AS on PTBP1. We found that knocking down PTB-AS using two different siRNAs in T98G, U87MG, and A172 glioma cell lines effectively downregulated PTBP1 at both the RNA and protein levels (Figures 2D, S3B, and S3C). Overexpressing PTB-AS in these three glioma cell lines resulted in significant upregulation of PTBP1 mRNA and protein (Figures 2E and S3D). To exclude the possibility of nonspecific effects on other PTB family members, we aligned the 3′ UTRs of the four PTB family members and found that the similarity was only 19.3% (Figure S3E). Therefore, we concluded that the expression of PTB-AS correlated positively with PTBP1. Here, we showed that manipulation of PTB-AS expression affected PTBP1 expression at both the RNA and protein levels, indicating that PTB-AS could specifically regulate PTBP1 expression in glioma.

PTB-AS Contributes to Glioma Cell Proliferation and Migration *In Vitro* and *In Vivo*

We investigated the biological functions of PTB-AS and PTBP1 by detecting their effects on proliferation and migration of glioma cells. We altered the expression of PTB-AS or PTBP1 by transfecting glioma cells with siRNA or plasmids. RNA or protein expression was detected to confirm transfection efficiency (Figures S4A and S4B). We also overexpressed or reduced PTB-AS or PTBP1 with a stable lentivirus transfection strategy (Figure S4C), and the established stable U87MG cells were used for later functional studies. 3-(4,5-dimethylthiazol-2-yl)-5-(3-carboxymethoxyphenyl)-2-(4-sulfophenyl)-2H-tetrazolium (MTS; Owen's reagent) and colony-formation assays showed that decreasing the expression of either PTB-AS or PTBP1 significantly inhibited the growth of glioma cells, but overexpressing PTB-AS or PTBP1 partially abrogated this effect (Figures 3A, 3B, and S4D). However, flow cytometry analysis showed that the proportion of apoptotic cells was not obviously different compared with that of the control group (Figure S4E). Next, we studied whether PTB-AS could affect the migration of glioma cells. In the wound-healing assay, PTB-AS or PTBP1 knockdown or overexpressing cells were less motile or more dynamic than lenti-NC-infected cells at closing an artificial wound created over a confluent monolayer (48 and 72 h, $^{**}p < 0.01$; Figures 3C and S4F). Directional migration was examined by Transwell assay, and we observed that knockdown or overexpression of PTB-AS and PTBP1 dramatically inhibited or promoted the migration of glioma cells, respectively, compared with that of the control cells treated with shRNA or lenti-NC (Figures 3D and S4G). Next, we aimed to address the relevance of these features *in vivo*. Intracranial orthotropic xenografts were established by implanting approximately 5×10^5 U87MG cells stably expressing either shPTB-AS (lenti-shPTB-AS) or the negative control lentivirus (lenti-shNC). H&E staining revealed that the PTB-AS-silenced glioma cells formed smaller tumors than the control cells (Figure 3E). Moreover, the cells showed obvious increases in epithelial marker level and reductions in mesenchymal markers or in expression of EMT-related transcription factors after knockdown of PTB-AS, followed by the weaker signal of Vimentin when PTB-AS was downregulated *in vivo* (Figure 3F). These results demonstrated that PTB-AS contributes to glioma proliferation *in vitro* and *in vivo* and promotes the migration of glioma cells.

PTB-AS Binds to PTBP1-3′ UTR and Stabilizes PTBP1 mRNA

We performed a rescue experiment and found that overexpressing PTB-AS could upregulate the expression of PTBP1 under PTB-siRNA knockdown conditions. This change also reflected the functional level of glioma (Figures S5A–S5D). Under conditions in which robust PTB-AS elevated PTBP1 expression and influenced glioma cell proliferation and migration, we further investigated the molecular mechanism by which PTB-AS regulates the expression of PTBP1.

Since the location of lncRNAs generally determines their function, we performed (fluorescence) *in situ* hybridization ([F]ISH) and RNA fractionation of the nucleus and cytoplasm and showed that PTB-AS is mainly located in the cytoplasm, indicating the potential of post-transcriptional regulation (Figures 4A, 4B, and S5E). The reverse complementary sequence between PTB-AS and PTBP1 indicates that they may have a binding relationship. We then investigated whether PTB-AS could directly bind to the 3′ UTR of PTBP1. To detect the RNA duplex formed by PTB-AS and PTBP1, we performed an RNase protection assay (RPA). The results showed that multiple sites in the overlapping regions were protected from degradation, whereas the non-overlapping regions of PTBP1 and PTB-AS were almost completely degraded by RNase A (Figure 4C). This result indicated that significant proportions of PTB-AS indeed form RNA-RNA duplexes with PTBP1, possibly at the sites of the 3′ UTR genomic locus. The physical interaction between PTB-AS and PTBP1-3′ UTR was further validated by biotin-avidin affinity pull-down assays (brief flowchart shown in Figure 4D). Endogenous PTBP1 mRNA was

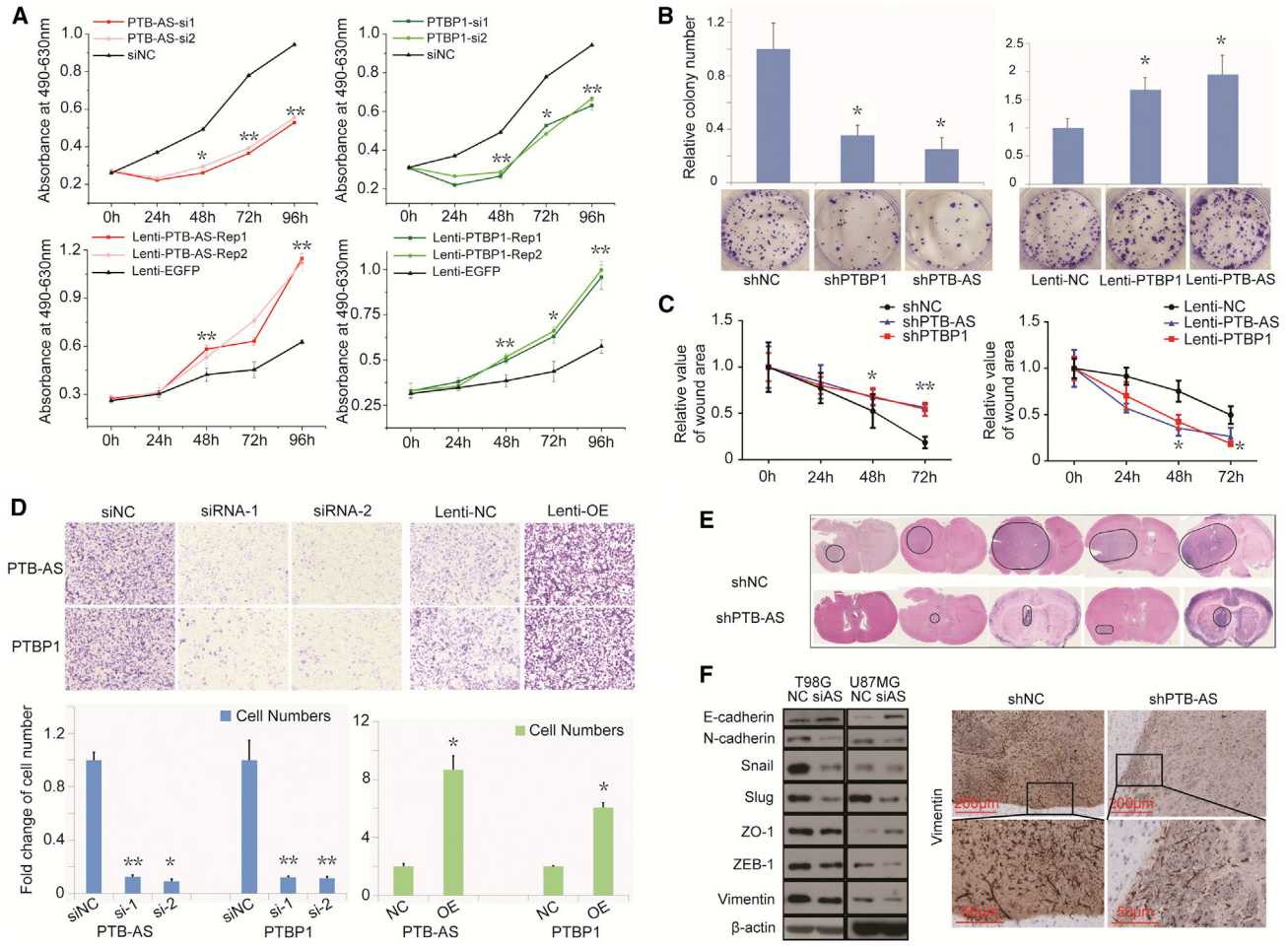

Figure 3. PTB-AS Could Significantly Promote the Proliferation and Migration of Glioma both *In Vitro* and *In Vivo*

(A and B) MTS and colony formation assays showing that PTB-AS, similar to PTBP1, promotes cell viability. (A) The growth curve of T98G cells after knocking down or overexpressing PTB-AS or PTBP1, following individual tests of the absorbance at 490 and 630 nm. (B) Colony formation images and bar charts of the number of colonies. Data are expressed as the mean ± SD, n = 5. *$p < 0.05$, **$p < 0.01$ (Student's t test). (C and D) Wound-healing assays and Transwell migration assays showing that PTB-AS and PTBP1 both promote the migration of glioma cells. (C) The relative area of the remaining open wound calculated in relation to that at time 0 h. (D) The graphs indicate the average number of cells per field of the indicated cell lines in migration assays. Data are the mean ± SD. *$p < 0.05$, **$p < 0.01$ (Student's t test). (E) *In vivo* assays were performed using shNC and shPTB-AS stable lentivirus infection U87MG cell suspensions (5×10^5 cells/5 μL). The cells were injected intracranially into five nude mice. H&E staining was processed after perfusion and paraffin preparation. The circles in the violet areas indicate the tumor. (F) An immunoblot analysis was performed to show the expression of mesenchymal markers, epithelial markers, and EMT-related transcription factors after knocking down PTB-AS, and representative immunohistochemistry was performed to detect Vimentin in shNC- and shPTB-AS-infected cells *in vivo*. Scale bars: 200 and 50 μm.

pulled down by a biotin-labeled PTB-AS probe transcribed *in vitro* and was detected by quantitative real-time PCR and agarose gel analyses. The biotin-labeled EGFP probe served as the negative control (Figures 4D and S5F). A dual-luciferase assay was used to examine whether PTB-AS could interact with PTBP1-3′ UTR. Our results revealed that knockdown of PTB-AS significantly reduced the luciferase activity, whereas the activity was restored by PTB-AS overexpression (Figure 4E). The above results indicated that PTB-AS could interact with PTBP1-3′ UTR through direct binding.

Next, we investigated the ability of PTB-AS to regulate the stability of PTBP1 mRNA. U87MG cells were treated with actinomycin D (Act D) to block transcription. Knockdown of PTB-AS decreased the half-life of PTBP1 mRNA from 8.7 to 5.3 or 3.4 h, whereas the half-life was substantially prolonged after overexpression of PTB-AS (Figures 4F and S5G), indicating that PTB-AS stabilizes PTBP1 mRNA. Thus, the data indicated that PTB-AS directly binds to the PTBP1-3′ UTR and strongly enhances the PTBP1 mRNA stability.

PTB-AS Masks the Binding Site of miR-9 in the PTBP1 3′ UTR Locus

miRNAs are ncRNAs that negatively regulate the expression of target genes by binding to their 3′ UTRs. In previous work,[25–27] PTBP1 was shown to be regulated by a series of miRNAs. Accordingly, we

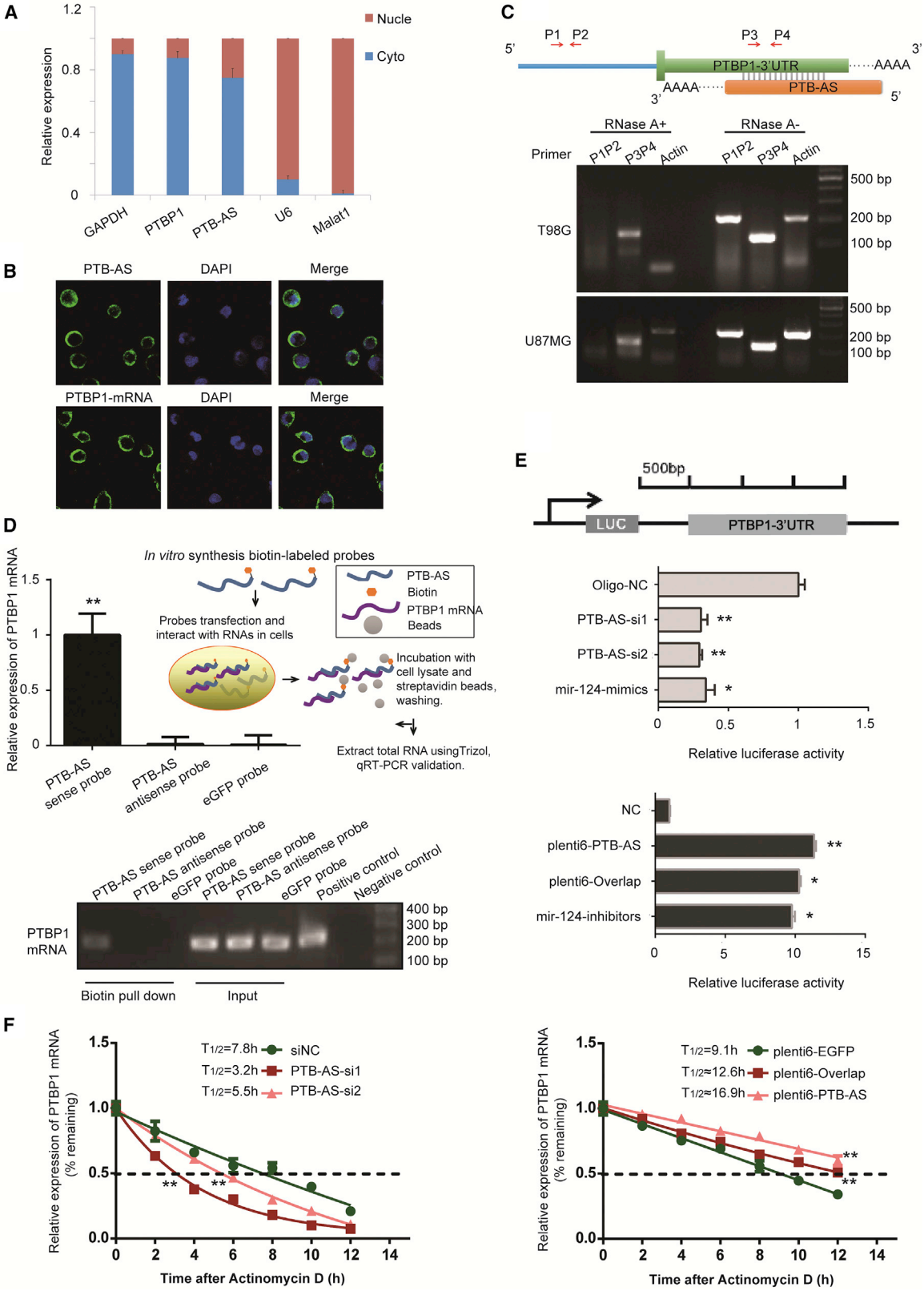

(legend on next page)

investigated whether the effect of PTB-AS on the stability of PTBP1 mRNA was also associated with miRNAs. We predicted miRNA binding at the PTBP1-3′ UTR by integrating the prediction results of the TargetScan, PicTar, Segal Lab, and MicroRNA.org webservers and finally obtained eight miRNAs, including miR-124 (as a positive control), which were reported to target PTBP1. The relative binding sites of the miRNAs are shown in Figure S6A.

All the results indicate that the relative luciferase activity of PTBP1-3′ UTR was significantly decreased when miR-124, -9, -133, -1, -153, -137, and -429 mimics (which resulted in miRNA overexpression) were transfected, compared with oligo-NC (Figure S6B). Thereafter, we performed western blot analysis to further confirm that the PTBP1 protein level was strongly reduced by overexpressing miR-124, -9, and -133 and slightly reduced by miR-429 (Figure S6C). We concluded that miR-9, -133, and -429 targeted PTBP1 and that inhibition of these molecules could significantly increase the expression of PTBP1 (Figures S6D and S6E). We observed that miR-9 and miR-133 were upregulated in glioma cells compared with normal astrocytes (Figures S6F and S6G), and other miRNAs were downregulated in glioma cells (data not shown). We mutated the binding site of miR-9 at the PTBP1-3′ UTR locus and found that mut-miR-9 could not bind to PTBP1-3′ UTR (Figure 5A). These results suggest that PTBP1 is the target gene of miR-9.

To explore the relationship between PTB-AS and miR-9 in regulating PTBP1, co-overexpression of PTB-AS and miR-9 was performed. We found that the expression level, or luciferase activity, of PTBP1 was obviously elevated when co-overexpression of PTB-AS and miR-9 was performed compared with overexpression of miR-9 (Figures 5B and 5C). However, miR-133 did not appear to be a candidate effector of PTBP1 (Figure S6H). We inhibited miR-9 and found that knocking down PTB-AS could significantly rescue the PTBP1 protein expression (Figure S6I). A biotin pull-down assay showed that miR-9 binding to PTBP1-3′ UTR was significantly reduced when PTB-AS was overexpressed. In contrast, enhanced miR-9 enrichment by PTBP1-3′ UTR was observed due to PTB-AS knockdown (Figures 5D and 5E). Unfortunately, changing the expression of miR-9 had no significant effects on the half-life of PTBP1-mRNA in glioma cells (Figures 5F and S6J) and on account of this unexpected phenomenon, we aimed to explore the major mechanism of PTBP1-mRNA stability. The results suggested that miR-9 could not target PTBP1 when PTB-AS was inhibited, because of masking of its binding site in PTBP1-3′ UTR.

SND1 Is Essential for PTB-AS Interaction with PTBP1 mRNA and Improvement of Its Stability

Antisense transcripts usually stabilize their target sense mRNAs through extended base pairing or physical interaction with mRNA-stabilizing proteins. While investigating the mechanism of PTB-AS-mediated stabilization of PTBP1-mRNA, we hypothesized that some RBPs may promote this double-strand RNA binding. We conducted an RNA pull-down assay and performed SDS-PAGE as well as silver staining, followed by mass spectrometry (MS) (Figure 6A). We aimed to identify proteins that bind to both PTB-AS and PTBP1-3′ UTR, and we obtained 87 peptides from 43 proteins (Table S5) from the intersection of the two groups after removing the background noise (Figure S7A).

Next, we chose the top three proteins that regulate RNA stability, which were SND1, ELAVL1 (Hu-antigen R [HuR]), and PABPC1 (PABP1). To evaluate these candidate proteins, we primarily performed nuclear and cytoplasmic extraction of U87MG cells and found that HuR, SND1, and PABP1 were detected in both the cytoplasm and the nucleus (Figures S7B and S7C). To validate the MS results, we performed an RNA pull-down assay, which showed that the biotin-labeled sense probes of both PTB-AS and PTBP1-3′ UTR could pull down these three proteins (Figure 6B).

We synthesized two-segment constitutive biotin-labeled RNA probes (A and B) of PTB-AS and PTBP1 mRNA, respectively,

Figure 4. PTB-AS Binds to the 3′ UTR of PTBP1 in the Cytoplasm and Promotes PTBP1 mRNA Stability

(A) Relative expression of PTB-AS and PTBP1 in nuclear RNA and cytoplasmic RNA was detected by quantitative real-time PCR in U87MG cells. GAPDH and U6 or MALAT1 were used as the cytoplasmic and nuclear loading controls, respectively. Data are shown as the mean ± SD, n = 3. (B) Fluorescence *in situ* hybridization for PTB-AS and PTBP1 mRNA on slides through T98G cells. All images show the same magnification (×100, with oil-immersion lens). Scale bar: 100 μm. (C) A ribonuclease protection assay (RPA) was performed to identify the binding relationship between PTB-AS and PTBP1-3′ UTR. The diagram shows the primer position. P1P2 primers were located in the PTBP1-coding sequence region, and P3P4 primers were located in the PTBP1-3′ UTR where it overlapped with PTB-AS. RT-PCR was performed and showed the PCR products after treatment of glioma cells with RNase A. (D) Biotin-based RNA pull-down assays showed that PTB-AS bound to the PTBP1-3′ UTR. A schematic of the biotin pull-down process is shown on the right. U87MG cells were transfected with biotinylated full-length PTB-AS. The antisense probes or biotinylated EGFP acted as a negative control. PTBP1-3′ UTR expression levels were analyzed by quantitative real-time PCR, and PCR products were amplified by agarose gel electrophoresis. The positive control indicates the precise position of the target band and PCR product, which was performed with free cDNAs as the negative control. Data are shown as the mean ± SD of three independent experiments. *p < 0.05; **p < 0.01 (Student's t test). (E) Luciferase assays revealed that PTB-AS could interact with the 3′ UTR of PTBP1. U87MG cells were separately infected with PTB-AS-siRNAs or the plenti6-PTB-AS vector, accompanied with the luciferase constructs of PTBP1-3′ UTR-pcDNA3.1-Luc or pRL-TK plasmids. The miR-124 group acted as a positive control; this molecule was reported to bind to the PTBP1-3′ UTR. The relative luciferase activity was analyzed, and the data are shown as the mean ± SD of three independent experiments. *p < 005, **p < 0.01 (Student's t test). (F) The half-life experiments showed that PTB-AS stabilized PTBP1 mRNA. U87MG cells expressing control siRNA, PTB-AS siRNA or plasmids were treated with actinomycin D (5 μg/mL) for the indicated periods of time. Total RNA was purified and then analyzed by quantitative real-time PCR to examine the mRNA half-life of PTBP1. Half-life was calculated by using one-phase decay, and significant differences were calculated using one-way ANOVA. Data shown are the mean ± SD. n = 3. *p < 0.05; **p < 0.01 (two-tailed t test), and the analyses used nonlinear regression (one-phase decay curve fit) to determine the half-life.

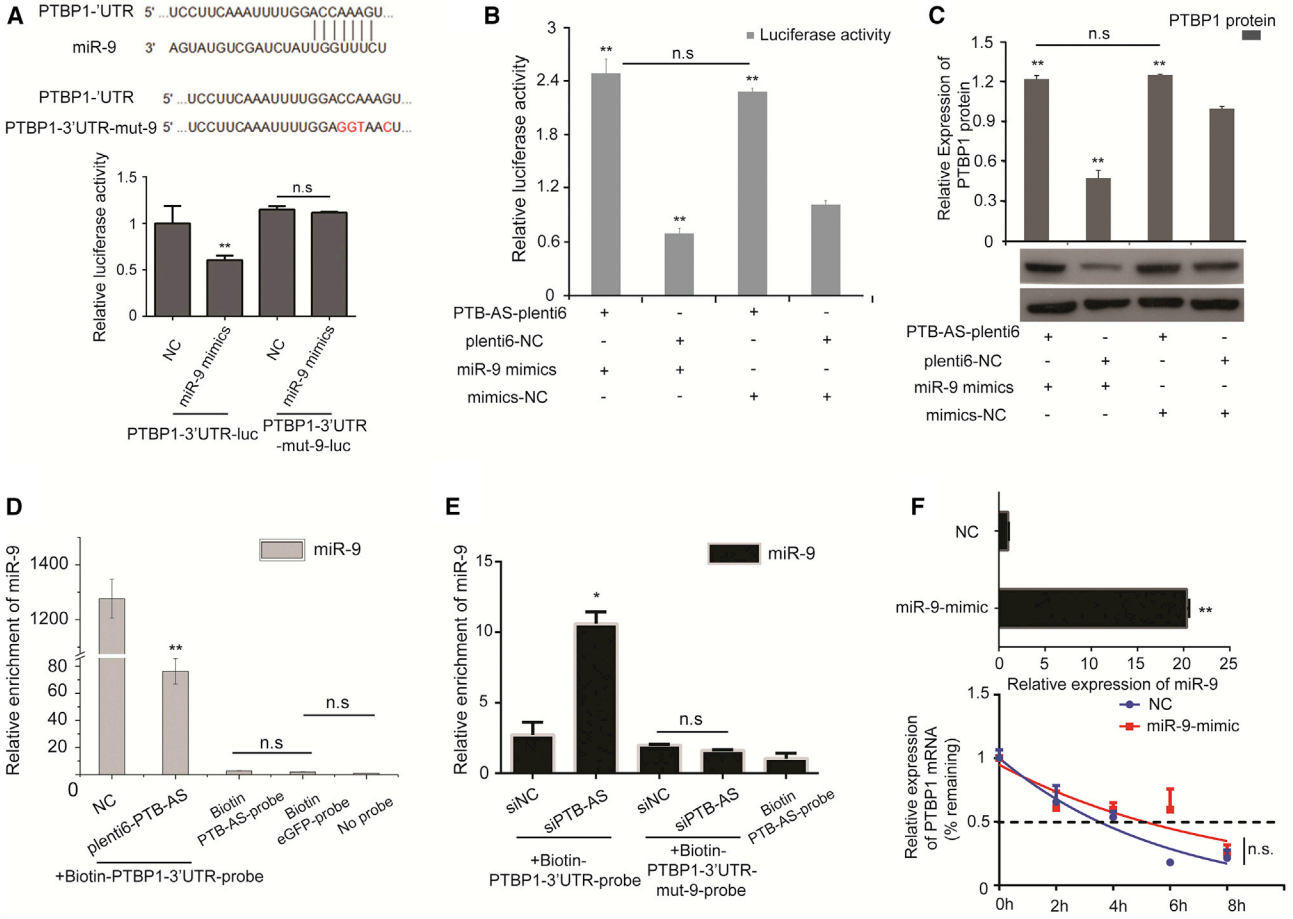

Figure 5. PTB-AS Contributes to the High Expression of PTBP1 by Masking the Binding Site of miR-9 in the PTBP1-3′ UTR

(A) PTBP1-3′ UTR-mut-9 was constructed to mutate the binding site of miR-9 in the PTBP1-3′ UTR. U87MG cells were separately infected with PTBP1-3′ UTR-luc and PTBP1-3′ UTR-mut-9-luc, all accompanied by transfection of the luciferase constructs of miR-9 mimic/mimic NC and pRL-TK plasmids. A luciferase assay was performed to analyze the relative luciferase activity, and the data are shown as the mean ± SD of three independent experiments. *$p < 0.05$; **$p < 0.01$ (Student's t test); n.s., non-significant. (B) U87MG was cotransfected with miR-9 mimic and plenti6-PTB-AS. Mimic-NC and plenti6-NC were the negative controls. Luciferase reporter assays were performed to validate the failure of miR-9 to target and negatively regulate PTBP1, and the failure was found to be caused by overexpression of PTB-AS. The relative luciferase activity value is shown as the mean ± SD, $n = 3$. *$p < 0.05$, **$p < 0.01$ (Student's t test). The results were from three biological replicates. (C) The western blot experiments were performed to validate the failure of miR-9 to regulate PTBP1, and the failure was found to be caused by overexpression of PTB-AS. Then, the results of the western blot assays were quantified by densitometry and are shown as the ratios of PTBP1 to β-actin protein levels (values in the right histogram). Relative values are shown as the mean ± SD, $n = 3$. *$p < 0.05$, **$p < 0.01$ (Student's t test). The results were from three biological replicates. (D and E) U87MG cells were transfected with biotinylated full-length PTBP1-3′ UTR probe or PTBP1-3′ UTR-mut-9 probe accompanied by plenti6-PTB-AS/plenti6-NC (D) or siPTB-AS/siNC (E). The biotinylated PTB-AS was the control. The EGFP probe and no-probe group were the negative controls. Forty-eight hours after transfection, cells were harvested for biotin-based pull-down assays. RNA extraction and RT-PCR were performed. miR-9 expression levels were finally analyzed by quantitative real-time PCR. Data are shown as the mean ± SD of three independent experiments. *$p < 0.05$, **$p < 0.01$ (Student's t test). (F) Half-life assay for PTBP1 mRNA after overexpression of miR-9. The mimic-NC or the miR-9 mimic was transfected into U87MG cells. Transcript decay curves were measured after transfection for 48 h when transcription was blocked by adding actinomycin D (5 μg/mL). Transcripts remaining relative to the control gene were assessed by quantitative real-time PCR. n.s., no significance. The analyses used nonlinear regression (one phase decay curve fit) to determine the half-life. Error bars, SD. The results were from three biological replicates.

followed by an RNA pull-down assay to identify the primary specific region binding to the candidate RBPs. Finally, we found that only SND1 tended to bind the overlapping region (segments PTB-AS-B and PTBP1-3′ UTR-B) compared with HuR or PABP1. Glyceraldehyde phosphate dehydrogenase (GAPDH) was used as a negative control, and no GAPDH protein was pulled down by any of the probes (Figure 6C).

SND1, HuR, and PABP1 are well-known stability regulators that usually improve the stability of target genes. We first altered the levels of SND1, HuR, and PABP1 and detected PTBP1 expression. We found that after these three candidate proteins were knocked down, PTBP1 showed various changes. Decreasing SND1 could significantly downregulate the PTBP1 mRNA level, and increasing SND1 strongly upregulated the PTBP1 mRNA level (Figures S7D and S7E). However,

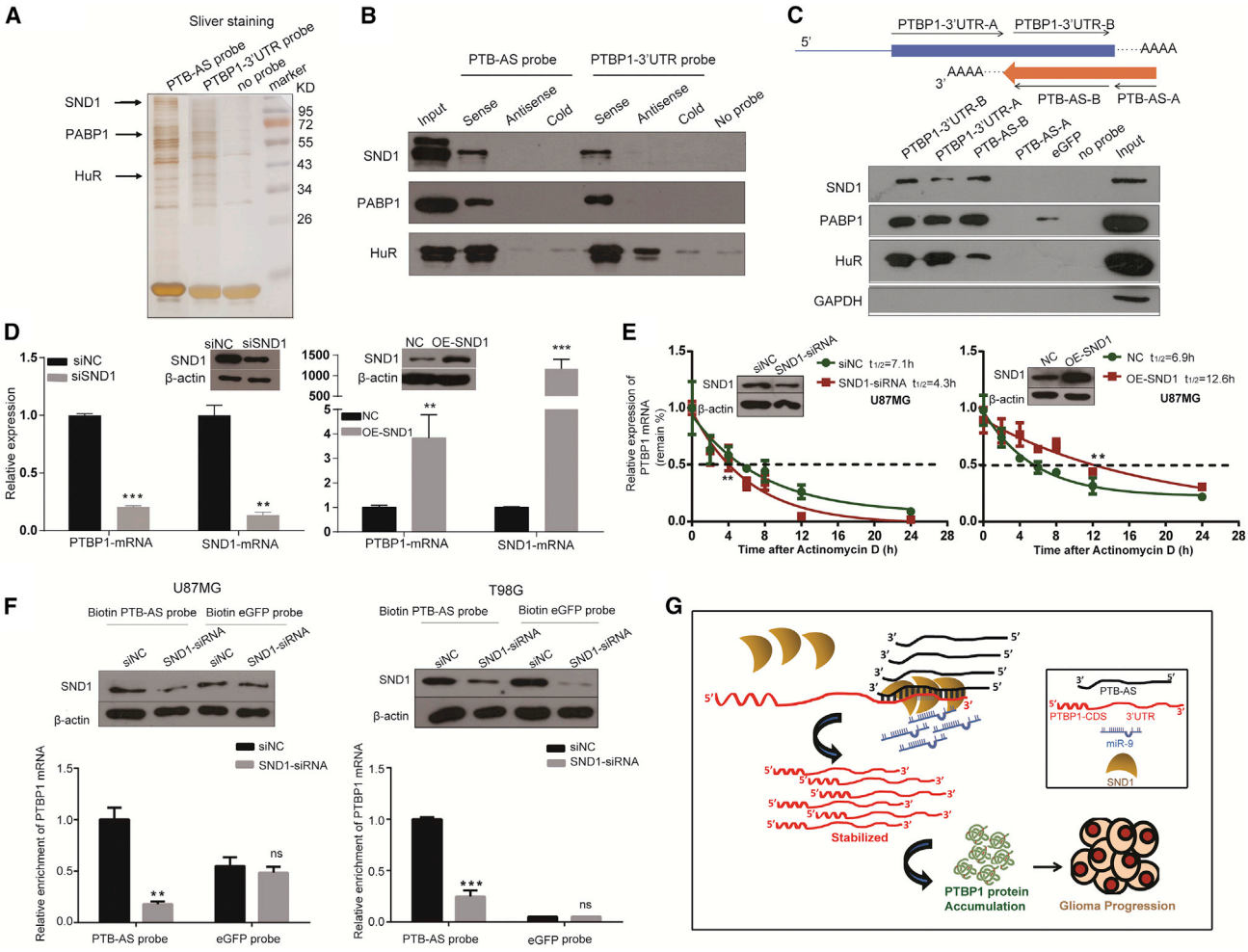

Figure 6. SND1, Which Is Necessary for the Interaction of PTBP1 mRNA and PTB-AS, Promotes PTBP1-mRNA Stability

(A) The search for RNA-binding proteins using affinity purification. Biotin-labeled probes corresponding to full-length PTB-AS or the 3′ UTR of PTBP1 were incubated with T98G cell lysates and analyzed by SDS-PAGE, and the proteins were then silver stained. The negative control group used no probe. The pull-down samples were analyzed by mass spectrometry. (B) RNA pull-down assays verified the binding capacity of candidate proteins to PTB-AS and PTBP1-3′ UTR in T98G cells. (C) Identification of specific regions in PTB-AS and PTBP1-3′ UTR bound by candidate proteins. The schematic representation of different segments of transcripts used as probes in affinity purification reactions is shown above. The biotin-labeled EGFP probe as the negative control probe did not bind to any proteins. The probes were incubated with T98G cell lysates. Input protein came from the cell lysates before probes were incubated. GAPDH, as a negative control protein, did not bind to any probes. (D) Knocking down or overexpressing SND1 dramatically changed the expression of PTBP1 mRNA. U87MG cells were infected with siRNA (or siNC) or plasmid (or empty plasmid) targeting SND1, to manipulate the expression of SND1. Western blot analysis demonstrated the SND1 protein level. PTBP1 and SND1 transcripts were measured by quantitative real-time PCR, n = 3. *p < 0.05; **p < 0.01, ***p < 0.001 (Student's t test). (E) U87MG cells expressing control siRNA or SND1 siRNA- or mock-vector (NC) or pcDNA4.0-SND1 plasmid (OE-SND1) were treated with actinomycin D (5 μg/mL) for the indicated periods of time. Total RNA was analyzed by RT-qPCR to examine the mRNA half-life of PTBP1. Data shown are the mean ± SD, n = 3. *p < 0.05, **p < 0.01 (two-tailed t test). The analyses used nonlinear regression (one-phase decay curve fit) to determine the half-life. (F) Biotin pull-down demonstrates that knockdown of SND1 weakens the binding between PTB-AS and PTBP1-3′ UTR. Cell lysates of U87MG cells and T98G cells expressing control siRNA or SND1-siRNA were incubated with *in vitro* synthesized biotin-labeled PTB-AS probe or EGFP probe for the biotin pull-down assays, followed by real-time qPCR analysis to examine PTBP1 mRNA levels. Total proteins from cell lysates were subjected to western blot with SND1 antibodies. Data shown are the mean ± SD (n = 3). *p < 0.05, **p < 0.01, ***p < 0.001 (Student's t test). (G) A schematic illustration of the proposed model depicting the role of PTB-AS in regulating PTBP1 mRNA stability. PTBP1 was significantly upregulated in glioma as a result of the dual-protection of PTB-AS; PTB-AS protected PTBP1 mRNA from inhibition by miR-9 through the masking effect; and SND1 dramatically stabilized PTBP1 mRNA through robustly enhancing the interaction of PTB-AS and PTBP1 mRNA.

PTBP1 mRNA expression was increased when PABP1 was reduced, and no significant differences were observed when HuR was knocked down (Figures S7F and S7G). We further investigated whether HuR, SND1, and PABP1 affect the stability of PTBP1 mRNA in glioma cells. SND1 substantially altered the half-life of PTBP1 mRNA in T98G and U87MG cells (Figures 6D and 6E). Interestingly, the half-life of PTBP1 mRNA did not change significantly after altering the expression of PABP1 or HuR. This result was not consistent

with the phenomenon of maintaining mRNA stability (Figures S7H and S7I).

Based on the above results, we hypothesized that SND1 may promote PTB-AS to interact with PTBP1 mRNA and enhance its stability. Previous reports showed that SND1 has a preference for binding proteins or double-stranded RNA[28] and can stabilize mRNA.[29] Thus, we further explored whether SND1 is essential for the binding of the double-stranded RNA complex. We performed RNA pull-down assays after knocking down SND1 in glioma cells. As shown in Figure 6F, the enrichment of PTBP1 mRNA by the PTB-AS probe was significantly reduced when SND1 was deleted, indicating that SND1 could influence the binding capacity of PTB-AS and PTBP1-3′ UTR. To summarize, we investigated whether SND1 could influence the mRNA level of PTBP1 by altering the binding of the PTB-AS and PTBP1 RNA molecules.

DISCUSSION

PTBP1, a multifunctional component of mRNA metabolism that affects splicing and mRNA stability, has been reported to be the first RBP that affects the invasive and rapid growth of glioma cells.[30] However, few detailed mechanisms underlying the upregulated PTBP1 in glioma have been reported. In this study, we identified a novel overexpressed antisense lncRNA, PTB-AS, in glioma cells and elucidated its functional molecular mechanism. In our model, PTB-AS directly binds to target PTBP1 mRNA through extended base pairs on the 3′ UTR and masks the binding sites of miR-9. The masking of the miR-9 binding sites by PTB-AS leads to the derepression of miR-9 on the PTBP1 protein. SND1 acts as a clamp to stabilize the double-stranded RNA complex and is essential for maintaining PTBP1 mRNA stability. In this way, PTBP1 expression is elevated by the combined effects of SND1, PTB-AS, and miR-9. Finally, the entire regulatory pathway substantially contributes to gliomagenesis (Figure 6G).

Several molecules have been shown regulate PTBP1, such as miR-124.[31,32] miR-124 influences tumorigenesis by regulating the PTBP1/PKM1/PKM2 pathway.[33] Furthermore, the lncRNA Tcl1 upstream neuron-associated (TUNA) is associated with PTBP1 and participates in recruiting the complex (hnRNP-K, NCL, and PTBP1) as a scaffold.[34] Another lncRNA, Pnky, could bind to, but not influence, PTBP1 and regulate the expression and alternative splicing of a core set of transcripts in neural stem cells.[35] Here, PTB-AS was shown to be a robust positive regulator of PTBP1 and is the first novel antisense lncRNA originating from the PTBP1 genomic locus to be investigated.

Growing evidence suggests that NATs play a key role in a range of human diseases, especially cancer.[36] For example, brain-derived neurotrophic factor (BDNF)-AS and BACE1-AS participate in regulating the neuronal outgrowth and differentiation and development of Alzheimer's disease through targeting their paired genes in the CNS, respectively.[37] Additionally, a NAT can also share the bidirectional regulatory relationship with its paired gene, such as WDR83 and its NAT DHPS, which function in gastric cancer.[38] Here, we identified a novel NAT lncRNA named PTB-AS with RACE, and northern blot analysis and revealed that the full-length PTB-AS is 923 nt with a Poly(A) tail structure, which has 595 nt of reverse complementary sequence with the 3′ UTR locus of PTBP1. Unlike TSLC1-AS, which was reported previously in glioma as a tumor suppressor,[39] PTB-AS is upregulated in tumor cell lines or tissues and functions as an oncogenic NAT. The high expression of PTB-AS significantly promoted proliferation and migration in glioma. The main cause of upregulated PTB-AS in glioma deserves further research and may be linked to RNA modification. Furthermore, given the increasing expression level of PTB-AS with increased malignancy in glioma, this molecule may serve as a potential biomarker for glioma.

The mechanisms by which NATs regulate gene expression are various and complex and are categorized as those that act in *cis* or in *trans*. Generally, NATs can interact with protein complexes as decoys, scaffolds, or tethers or guides; participate in the generation of endogenous siRNAs and miRNAs or modulation of mRNA stability; and mediate the stabilization of long-range chromosomal interactions.[40] We discovered that PTB-AS is coexpressed and colocalized with PTBP1 mRNA, and we speculated that it is a putative *cis*-regulatory factor. To investigate the regulatory mechanism of PTB-AS on PTBP1, we manipulated the expression of PTB-AS, demonstrating that it is closely associated with PTBP1 mRNA stability. Our findings suggested that PTB-AS may stabilize sense PTBP1 mRNA through extended base pairing at the PTBP1 3′ end. Further mechanistic investigation revealed that miR-9 and SND1 are involved in this process.

NATs regulate sense genes mainly through direct antisense-sense RNA interactions, and the most common pattern is RNA masking, in addition to RNA editing, transcriptional or RNA interference and chromatin changes.[41] The "masking" of NATs provides a physical barrier against factors that may induce splicing or influence the stability of sense genes. In our study, we found that PTB-AS protects PTBP1 mRNA by masking the miR-9 binding site. Although this overlapping area can be targeted by several miRNAs, miR-9, with a high expression level in glioma cells, seems to be a key miRNA involved in the regulatory network. Evidence has proven that miR-9 is upregulated by CAMP responsive element binding protein (CREB) in glioma cells and negatively regulates the proliferation and migration of glioma.[42] In addition, miR-9 could substantially enhance temozolomide resistance and tumor recurrence in GBM through targeting PTCH1, which negatively regulates Sonic Hedgehog (SHH) signaling.[43,44] Considering the inhibitory effect of miR-9 in glioma cells, we conjectured and verified that miR-9 could negatively interfere with PTBP1 and that the binding site of miR-9 in PTBP1-3′ UTR is masked by PTB-AS in glioma. This type of mechanism can be referred to as an "occupation effect," which has been reported to influence the function of miRNAs.[45] This is the first investigation to show that miR-9 regulates the expression of PTBP1 in humans, especially in cancer.

However, we cannot explain whether the space-occupying effect of PTB-AS on miR-9 has selectivity yet. The in-depth mechanism of the high expression of miR-9, PTB-AS, and PTBP1 mRNA remains to be further verified.

SND1 is a multifunctional protein that is upregulated in different cancers. SND1 was initially characterized as a transcription coactivator that interacts with several specific transcription factors, including c-Myb,[46] STAT6, and STAT5.[28] SND1 is also involved in RNA maturation, including but not limited to spliceosome assembly, pre-mRNA splicing,[47,48] and RNA stability.[29] In this study, we investigated whether SND1 possesses a new function. SND1 could stabilize the combination of lncRNA PTB-AS and its complementary mRNA.

Structurally, SND1 contains four repeats of staphylococcal nuclease-like domains (SN1–SN4) at the N-terminal followed by a Tudor domain and a fifth truncated SN domain at the C-terminal end.[49] This particular structure allows the protein to interact with nucleic acids, individual proteins, and protein complexes in a promiscuous manner. Interestingly, our results showed that compared to HuR or PABP1, SND1 showed more specific binding to the double-stranded RNA structure formed by PTB-AS and PTBP1-3′ UTR in RNA pull-down assays. Thus, we hypothesized that the SN3 and SN4 domains of SND1 may act as a clamp to affect the binding of the duplex structure of PTB-AS and PTBP1-mRNA, which assists PTB-AS in regulating its target mRNA stability. Our results showed that HuR has a regulatory effect on PTBP1 mRNA stability, and thus, HuR cannot be ruled out completely. These results indicate that the regulation of PTBP1 is more complicated than we had anticipated, and the new functions of PTB-AS and RBPs need to be characterized.

Precision medicine is urgently needed. Therapeutic agents that potentially target lncRNAs mostly function via reducing the intracellular transcript levels of lncRNAs or attenuating their activities and molecular functions in cancer cells.[50] Furthermore, potential pharmacological principles have suggested the application of NATs in gene therapy for glioma, and several strategies have been designed to use NATs as potential drug targets.[51] Historically, lncRNAs can be easily inhibited by oligonucleotide-based drugs (ASO and others), and these molecules seem preferable to undruggable proteins for cancer therapy.[52] The presence of lncRNAs (which show specific expression, complicated degradation pathways and little conservation) in biological fluids and their deep involvement in tumorigenesis make them ideal candidates for the development of efficient diagnostic assays;[53,54] therefore, the use of PTB-AS as a diagnostic marker will be easier and more sensitive than PTBP1 protein (antibody-based detection) because glioma tissue samples are generally limited. In addition, PTB-AS could be used for liquid biopsy based on RNA detection in peripheral blood or cerebrospinal fluid. Finally, the secondary structure of PTB-AS may offer clues for designing inhibitor-targeted PTBP1 molecules for glioma therapy applications. To summarize, our findings demonstrate the potential underlying mechanism of PTB-AS in the regulation of PTBP1 expression in glioma and possibly provide a therapeutic application.

MATERIALS AND METHODS

Cell Culture

The two human normal astrocyte cell lines (HA-c and HA-sp) and glioma cell lines (T98G, U87MG, A172, HS-683, SF-126, SF-763, SF-767, SHG-44, CCF-STGG1, H4, LN-18, LN-229, and U118MG) mentioned in this article were purchased from the American Type Culture Collection (ATCC). The glioma cell line U251 was ordered from the Cell Center of Peking Union Medical College. T98G and U87MG were maintained in modified Eagle's medium including 1 mM sodium pyruvate, 1% (vol/vol) non-essential amino acids (NEAA), 10% (vol/vol) fetal bovine serum (FBS), 5 mM L-glutamine, 100 U/mL penicillin, and 100 mg/mL streptomycin. The other cell lines were maintained in DMEM supplemented with 10% FBS, 5 mM L-glutamine, and dual antibiotics. The NHA cell line was purchased from the Lonza group and cultured with medium and reagents from Clonetics. The other HA cell line was purchased from ScienCell Research Laboratories and cultured with astrocyte medium (cat. no. 1801; ScienCell).

Tumor Tissues from Clinical Cases

A total of 83 glioma tissue samples and 6 control brain tissues (from the Department of Neurosurgery, Beijing Tiantan Hospital) were included in this research. Malignancy grade (14 samples were grade II, 25 samples were grade III, and 44 samples were grade IV) was defined according to the guidelines of the World Health Organization (WHO). The use of these human materials was in accordance with the policies of the institutional review board at Beijing Tiantan Hospital.

RACE

A172 total RNA was used to generate RACE-ready cDNA by using the commercial kit 5′&3′ RACE System for Rapid Amplification of cDNA Ends (cat. nos. 18374-058 and 18373-019; Invitrogen), according to the manufacturer's protocol. cDNA ends were amplified with Universal Primer Mix and gene-specific primers. Placental RNA and receptor-specific primers provided by the manufacturer were used as controls. To ensure that we obtained distinct bands for the primary PCR, we performed a "nested PCR" with the nested universal primer and nested gene-specific primers shown in Table S4. Although the sample had a 3′ Poly(A) tail, for regent, we used the Poly(A) polymerase (cat. no. TAK2180; TaKaRa) to add a poly-adenylated tail to the total RNA of 3′ RACE. PCR products were then run in a 1.5% agarose gel, and DNA was extracted, cloned in the pGEM-T plasmid, and sequenced by Invitrogen.

Northern Blot Analysis

Total RNA, extracted using TRIzol reagent from U87MG glioma cells, was subjected to northern blot assays. The PTB-AS-specific DNA sequence (341 nt) was cloned into the pGEM-3zf vector. An RNA probe with a length of 341 nt was generated using digoxin (Roche) and the Riboprobe *in vitro* transcription labeling system (TaKaRa). The sense and antisense RNA probes were designed according to the principle that minimized nonspecific hybridization against mRNAs after homology searches using BLAST. A total of 3–10 μg

of the indicated total RNA was subjected to formaldehyde gel electrophoresis and transferred to a Biodyne Nylon membrane (Pall, NY, USA). A digoxin-labeled PTB-AS sense or antisense probe was prepared. All of the procedures were strictly performed according to the manufacturer's instructions (cat. no. 12039672910; Roche).

Identification of RNA Copies Using Absolute qPCR

First, the full-length of PTB-AS and PTBP1-CDS were cloned to pGEMT-3zf, then *Bam*HI was used to digest and form the linearized plasmid template A (a serious cascade dilution rate was designed as 1, 1:10, 1:100, and 1:1,000). The standard curve was made according to the starting cycle value (Ct), using a template and aiming at indicating the good linear relationship between the template and the Ct value. Template B was reverse transcribed cDNAs from HA, T98G and U87MG cell lines ($\sim 10^4$ cells), and cDNAs were amplified once to form the double-stranded template in the same way as the linearized plasmid template. Fluorescence qPCR was performed using template A and B together to identify the starting copy numbers of PTB-AS and PTBP1. The calculating formula is as follows (Equation 1):

$$\text{Starting copy numbers (copies/}\mu\text{L)} = 6.02 \times 10^{23}\text{(copies/mol)} \times \text{concentration of linearized plasmid (g/}\mu\text{L)/molecular weight of plasmid (g/mol).} \quad \text{(Equation 1)}$$

RNA Extraction and Quantitative Real-Time PCR

All total RNAs were isolated from corresponding treated cells with TRIzol reagent (Invitrogen) and were reverse transcribed by gene-specific primers (for PTB-AS), oligo(dT) primer (for PTBP1) or stem-loop Reverse-Transcript-PCR primer (for mature miRNAs). The RT process was performed (TransGene) to generate cDNA templates, strictly according to the manufacturer's instructions. Quantitative real-time PCR was performed with a SYBR Green-containing PCR kit (TaKaRa), and the IQ5 sequence detection system (Applied Biosystems) according to the manufacturer's instructions. RNA input was normalized to the level of human GAPDH mRNA and U6 snRNA (for miRNA detection) to determine relative gene expression. The primer sequences used for RT-PCR and quantitative real-time PCR are listed in Table S4.

Western Blot Analysis

All of the tumor tissues and treated or untreated glioma cells were harvested using TNTE lysis buffer (pH 7.4), containing 50 mM Tris-HCl, 150 mM NaCl, 0.5% Triton X-100, 1 mM EDTA, 1 mM Na_3VO_4, 25 mM NaF, and 10 mM $Na_4P_2O_7 \cdot 10\ H_2O$ and protease inhibitors (5 μg/mL PMSF, 0.5 μg/mL leupeptin, 0.7 μg/mL pepstatin, and 0.5 μg/mL aprotinin). Proteins for immunoblotting were run in 8%–15% SDS-PAGE gels (Invitrogen) and transferred to nitrocellulose membranes. The nitrocellulose membranes were blocked with 5% skim milk in Tris-buffered saline-Tween 20 (TBS-T; 20 mM Tris-HCl [pH 7.4], 150 mM NaCl, 10 mM KCl, and 0.1% Tween 20) for at least 1 h. Antibodies were added in TBS-T containing 5% skim milk, and the blots were washed with TBS-T. Immunoblot signals were developed with an enhanced chemiluminescence reagent (GE Healthcare Bio-Sciences). The antibodies used in this study were as follows: rabbit anti-human PTBP1 (provided by our lab, 1:4,000 dilution) and mouse anti-human β-actin (1:8,000 dilution; cat. no. A5441; Sigma, USA).

Plasmids, shRNA, Lentivirus, siRNAs, and Transfection

The target sequences of siRNAs for PTB-AS and PTBP1 were designed and synthesized by Invitrogen, and the mimics of all miRNAs were synthesized by GenePharma. The cDNA target sequences of short hairpin RNAs (shRNAs) for PTBP1 were purchased from Thermo Fisher Scientific (cat. no. TRCN0000001062), and shRNA-oligos for PTB-AS were designed by us and synthesized by Invitrogen. The full-length PTB-AS and PTBP1-CDS and their overlapping region were cloned into the plenti6 vector. The PTBP1-3′ UTR was cloned into the pcDNA3.1-luc vector. The plasmid used to prepare the probe was segment-pGEM-3zf. All of the plasmids were purified using the EndoFree Plasmid Maxi Kit (QIAGEN) and transfected into T98G, U87MG, A172, or 293T cells using Lipofectamine 2000 (Invitrogen). siRNAs were transfected into glioma cell lines using INTERFERin (PolyPlus) at a final concentration of 100–200 nM.

Growth, Colony Formation, Fluorescence Activated Cell Sorting, Transwell Migration, and Scratch Wound-Healing Assays

T98G, U87MG, and A172 glioma cell line growth was assayed by using the standard MTS method. Twenty-four hours after transfection, the cells were maintained in serum-containing medium, and the number of surviving cells was determined by using the MTS method (G111B; Promega). In colony-formation assays, transfected or infected cells were plated in 12-well plates at 3,000 cells per well. Ten to 14 days later, the cell colonies were stained and counted. For apoptosis analysis, the transfected cells were harvested and assessed for apoptosis using an Annexin V-FITC-PI dual-staining kit (Abchem) by flow cytometry. In the Transwell migration assay, 5×10^4 to 1×10^5 T98G, U87MG, and A172 cells were plated on 8 μm Transwell filters (Corning) after transfection for approximately 24∼48 h. The cells were cultured with serum-free medium for 12 h and induced to migrate toward medium containing 10% FBS for about 24 h in the CO_2 incubator. We use a cotton swab to remove non-migrating cells. The cells outside the well were fixed and stained using 0.1% crystal violet. An ix71 inverted microscope (Olympus) was used to count and image migrating cells. We chose four random fields to count and calculate the average number of cells. Scratch wound-healing assays were performed, and after the infected U87MG cells reached a confluence of 90% to 95%, a pipette tip was used to create the scratch wound. The suspended cells were removed by two washes with 1× PBS after scratching, following by addition of fresh medium to the cells. The cells were imaged at 0, 24, 48, and 72 h after scratching, and the migration status was calculated by measuring the wound areas with Nikon imaging software.

Xenograft Model in Nude Mice

The lentivirus-infected U87MG cells (1×10^7) in 100 μL 1× PBS were implanted into 4-week-old BALB/c athymic nu/nu mice (Vital River).

Intracranial orthotopic xenografts were established by implanting 5×10^5 lenti-U87MG stably transfected cells. The shNC-U87MG and shPTB-AS-U87MG stable transfectants were constructed by our lab. First, the BALB/c athymic nu/nu mice were anaesthetized, and we stereotactically implanted stably infected U87MG cells into the third ventricle (approximately 2 mm lateral and 0.5 mm anterior to the bregma; depth 1.5 mm from the dura). Approximately 1 month later, tumor size was quantified by H&E staining after perfusion. Paraffin-embedded sections of tumors were subjected to standard H&E staining.

ISH and FISH

Following the subcloning protocol, antisense digoxygenin-labeled probes were prepared and hybridized against fixed T98G, U87MG, and A172 cells. Wholemount ISH of glioma cell lines was performed, as previously described, with some modifications. The cells were observed with an optical microscope (ECLIPSE Ni-E; Nikon) and a confocal laser microscope (FV1000; Olympus).

Isolation of Cytoplasmic and Nucleic Cell Protein and RNA

Nuclear and cytoplasmic isolation was performed on U87MG cells using the SurePrep Nuclear or Cytoplasmic RNA Purification Kit (cat. no. BP2805-25; Fisher Bioreagents), according to the manufacturer's protocols. Then, quantitative real-time PCR was used to identify the RNA levels. In summary, we used an equivalent volume of nuclear and cytoplasmic RNAs to perform RT-PCR to generate the cDNA template. Nuclear and cytoplasmic enrichment ratios were calculated to display the final result.

RNA Pull-Down Assays and Silver Staining

We collected the glioma cell lysate using nuclear and cytoplasmic isolation methods and then combined the cytoplasm and nucleic components. First, streptavidin sepharose was pretreated using RNA binding buffer (50 mmol/L KCl, 1.5 mmol/L $MgCl_2$, 10 mmol/L HEPES [pH 7.5], 0.5% NP40, 2 mmol/L DTT, 1 mmol/L EDTA, 100 U/mL RNase inhibitor [40 U/μL], protease inhibitor, 100 μg/mL tRNA, and 400 μmol/L vanadyl ribonucleoside complexes). Then, we subpackaged 100–300 μL cell lysates for each sample and added 500–700 μL RNA binding buffer and 1–2 μg biotin-labeled probe. The mixture was well blended and formed an RNA-protein complex after incubation at 30°C for 30 min. Then, the RNA-protein mixture was combined with streptavidin sepharose, which had been treated and washed previously, followed by inverting shaking incubation at room temperature for 50 min. Finally, we used 30 μL PBS and 20 μL 6× loading buffer to suspend the streptavidin sepharose after six strict washes with RNA washing buffer (50 mmol/L KCl, 1.5 mmol/L $MgCl_2$, 10 mmol/L HEPES [pH 7.5], and 0.5% NP40) and performed silver staining, MS, or western blot assays. Briefly, the silver staining assay was conducted as follows: an SDS-PAGE gel was run using the protein obtained through RNA pull-down and washed two times for 5 min each with ultrapure water; then, the gel was fixed (50% water:40% methanol:10% acetic acid solution) two times for 15 min each at room temperature or overnight at 4°C; the gel was washed using sensitization solution (30% ethanol, 2.72 g/40 mL sodium acetate, and 1.3 g/40 mL $Na_2S_2O_3$) two times for 15 min each, and then washed 5 times for 5 min each in ultrapure water; the gel was incubated using stain working solution (0.1 g $AgNO_3$/40 mL) for 30 min in darkness; the gel was washed using Developer Working Solution (1 g/40 mL Na_3CO_3; 10 μL 37% formaldehyde [40 mL]), and *in situ* observation was performed; and finally, the gel was washed with EDTA solution (10 mM) and photographed.

Liquid Chromatography-Tandem MS and Data Analysis

The lyophilized samples were redissolved in 0.1% formic acid (buffer A) before MS analysis. The samples were analyzed on a self-packing RP C18 capillary liquid chromatography (LC) column (75 μm × 100 mm, 1.9 μm). The eluted gradient was 5%–30% buffer B (0.1% formic acid, 99.9% ACN; flow rate, 0.3 μL/min) for 40 min. MS data were acquired in TripleTOF MS, using an ion spray voltage of 3 kV, curtain gas of 20 PSI, nebulizer gas of 30 PSI, and an interface heater temperature of 150°C. The precursors were acquired in 500 ms ranging from 350 to 1,250 Da, and the product ion scans were acquired in 50 ms ranging from 250 to 1,800 Da. A rolling collision energy setting was used. A total of 30 product ion scans were collected if they exceeded a threshold of 125 counts per second (counts/s) and with a +2 to +5 charge state for each cycle. The tandem MS (MS/MS) spectra were searched against the UniProt human database from the Uniprot website (https://www.uniprot.org:443/) using Proteinpilot software suite (v4.0, Absciex). Trypsin was chosen for cleavage specificity, with two being the maximum number of allowed missed cleavages. Carbamidomethylation of cysteine was set as fixed modifications. The searches were performed using a peptide tolerance of 0.05 Da and a product ion tolerance of 0.05 Da. A 1% false-positive rate at the protein level was used as a filter, and each protein contained at least two unique peptides.

RPA

T98G, U87MG, and A172 cells were cultured in 10 cm dishes and isolated and purified into nuclear and cytoplasmic components. We performed RNA extraction from the nuclear and cytoplasmic mixture using TRIzol regent and digested the samples with DNase I to remove DNA contamination. The purified RNA was treated with RNase A (Ambion) to digest the single-stranded RNAs in digestion buffer. Following RT-PCR, agarose gel analysis was performed to identify the binding ability and the protective effect of PTB-AS on PTBP1.

Biotin Pull-Down Assay

U87MG cells were transfected with the biotinylated PTB-AS or the PTBP1-3′ UTR probe (50 nM) for 48 h. Then, we harvested the cells using lysis buffer (20 mM Tris [pH 7.5], 200 mM NaCl, 2.5 mM $MgCl_2$, 0.05% Igepal, 60 U/mL, SUPERase-In [TaKaRa], 1 mM DTT, and protease inhibitors [Roche]), and the lysate was placed on ice for 10 min. Fifty microliters of lysates was used as the input control. The remaining lysates were incubated with pre-prepared R10-Flammable streptavidin magnetic beads (GE Healthcare). To prevent nonspecific binding to RNA or protein complexes, we mixed the beads with RNase-free bovine serum albumin (BSA)

and yeast tRNA (both from Sigma) when incubated in blocking lysates at 4°C for 3 h to generate probe-coated magnetic beads. Then, the samples were washed twice with ice-cold lysis buffer, three times with low-salt buffer (0.1% SDS, 1% Triton X-100, 2 mM EDTA, 20 mM Tris-HCl [pH 8.0], and 150 mM NaCl), and once with high-salt buffer (0.1% SDS, 1% Triton X-100, 2 mM EDTA, 20 mM Tris-HCl [pH 8.0], and 500 mM NaCl). The bound RNAs were extracted and purified with TRIzol reagent. The RNA complexes bound to the beads were eluted and extracted for quantitative real-time PCR.

Dual-Luciferase Reporter Assays

PTBP1-3′ UTR was amplified and cloned into pcDNA3.1-luc with the restriction endonuclease sites of *Xho*I and *Xba*I. U87MG cells (90% confluence) were cultured in 24-well plates (Corning). Then, PTB-AS-siRNAs, siNC, PTB-AS-plenti6, plenti6-EGFP, miRNA mimics or mimic-NC were cotransfected with PTBP1-3′ UTR-luc and pRL-TK (the internal control plasmid constitutively expressing *Renilla* luciferase) by Lipofectamine 2000-mediated gene transfer. The relative luciferase activity was normalized to *Renilla* luciferase activity 48 h after transfection. The detailed procedures were performed according to the manufacturer's instructions. All transfection experiments were performed in triplicate.

Half-Life Assay

U87MG cells and T98G cells were treated with siRNAs targeting PTB-AS or SND1, PABP1, HuR, and control non-targeting siRNA or PTB-AS-plenti6 and pcDNA4.0-SND1 overexpression constructs and plenti6-EGFP vector or mock vector. For analysis of RNA stability, immediately after transfection for 36 h, cells were treated with Act D (5 μg/mL; Sigma-Aldrich), a drug that inhibits RNA polymerase to block the synthesis of new RNA. The cells were then harvested for total cellular RNA isolation at 0, 1, 2, 4, 6, 8, 10, 12, and 24 h after the addition of Act D and analyzed to measure the half-life of PTBP1 mRNA by quantitative real-time PCR. We performed three independent experiments for each data point.

Bioinformatics Analysis and miRNA Target Prediction

The coding potential of PTB-AS was predicted using the CPC and Coding Potential Assessment Tool (CPAT). The University of California, Santa Cruz (UCSC), gene browser was used to analyze the relative gene locus, transcription activity, histone modification, and other information on PTB-AS and PTBP1. Four target prediction databases (TargetScan, PicTar, Segal Lab, and MicroRNA.org) were used to analyze the potential target miRNAs of PTBP1.

Statistical Analysis

All experiments were performed at least in triplicate, and the data are expressed as the mean ± SD. All statistical analyses were performed with SPSS 13.0 for Windows (SPSS Inc., Chicago, IL, USA), and the data were analyzed with Student's t test or by one-way ANOVA. The results were considered statistically significant at $p \leq 0.05$. The Wilcoxon test was used to evaluate the statistical significance of the difference in the expression of PTB-AS or PTBP1 mRNA and protein. The chi-square test was used to determine correlations between PTB-AS and PTBP1 expression.

SUPPLEMENTAL INFORMATION

Supplemental Information can be found online at https://doi.org/10.1016/j.ymthe.2019.05.023.

AUTHOR CONTRIBUTIONS

L.Z., Q.W., W.H., and X.P. conceived and designed the experiments; L.Z., Q.W., Y.Q., X.R., F.W., L.L., and J.Z. performed the experiments; L.Z. and Q.W. mainly analyzed the data; B.Y., W.L., J.Z., T.J., B.Q., and J.Y. contributed reagents, materials, and analysis tools; and L.Z. and Q.W. wrote the manuscript.

CONFLICTS OF INTEREST

The authors declare no competing interests.

ACKNOWLEDGMENTS

This work was supported by grants from the National Key Research and Development Program of China (2016YFC0902500, 2016YFC0902502, and 2016YFA0100702), and National Sciences Foundation of China (31671316 and 31670789), CAMS Innovation Fund for Medical Sciences (CIFMS; 2016-I2M-1-001, 2016-I2M-2-001, 2016-I2M-1-004, 2017-I2M-2-004, 2017-I2M-3-010, and 2017-I2M-1-004). We thank members of the National Laboratory of Medical Molecular Biology (China) for their valuable input and support throughout this study. We thank Xiaochao Tan from MD Anderson Cancer Center and Xue Yuanchao from the Institute of Biophysics, Chinese Academy of Sciences, for reviewing and editing the manuscript.

REFERENCES

1. Perdomo-Pantoja, A., Mejía-Pérez, S.I., Gómez-Flores-Ramos, L., Lara-Velazquez, M., Orillac, C., Gómez-Amador, J.L., and Wegman-Ostrosky, T. (2018). Renin angiotensin system and its role in biomarkers and treatment in gliomas. J. Neurooncol. *138*, 1–15.

2. Omuro, A., and DeAngelis, L.M. (2013). Glioblastoma and other malignant gliomas: a clinical review. JAMA *310*, 1842–1850.

3. Ouédraogo, Z.G., Biau, J., Kemeny, J.L., Morel, L., Verrelle, P., and Chautard, E. (2017). Role of STAT3 in Genesis and Progression of Human Malignant Gliomas. Mol. Neurobiol. *54*, 5780–5797.

4. Uren, P.J., Vo, D.T., de Araujo, P.R., Pötschke, R., Burns, S.C., Bahrami-Samani, E., Qiao, M., de Sousa Abreu, R., Nakaya, H.I., Correa, B.R., et al. (2015). RNA-Binding Protein Musashi1 Is a Central Regulator of Adhesion Pathways in Glioblastoma. Mol. Cell. Biol. *35*, 2965–2978.

5. Dreyfuss, G., Kim, V.N., and Kataoka, N. (2002). Messenger-RNA-binding proteins and the messages they carry. Nat. Rev. Mol. Cell Biol. *3*, 195–205.

6. Yang, B., Hu, P., Lin, X., Han, W., Zhu, L., Tan, X., Ye, F., Wang, G., Wu, F., Yin, B., et al. (2015). PTBP1 induces ADAR1 p110 isoform expression through IRES-like dependent translation control and influences cell proliferation in gliomas. Cell. Mol. Life Sci. *72*, 4383–4397.

7. Han, W., Xin, Z., Zhao, Z., Bao, W., Lin, X., Yin, B., Zhao, J., Yuan, J., Qiang, B., and Peng, X. (2013). RNA-binding protein PCBP2 modulates glioma growth by regulating FHL3. J. Clin. Invest. *123*, 2103–2118.

8. Izaguirre, D.I., Zhu, W., Hai, T., Cheung, H.C., Krahe, R., and Cote, G.J. (2012). PTBP1-dependent regulation of USP5 alternative RNA splicing plays a role in glioblastoma tumorigenesis. Mol. Carcinog. *51*, 895–906.

9. Sawicka, K., Bushell, M., Spriggs, K.A., and Willis, A.E. (2008). Polypyrimidine-tract-binding protein: a multifunctional RNA-binding protein. Biochem. Soc. Trans. *36*, 641–647.

10. Makeyev, E.V., Zhang, J., Carrasco, M.A., and Maniatis, T. (2007). The MicroRNA miR-124 promotes neuronal differentiation by triggering brain-specific alternative pre-mRNA splicing. Mol. Cell *27*, 435–448.

11. Chen, M., Zhang, J., and Manley, J.L. (2010). Turning on a fuel switch of cancer: hnRNP proteins regulate alternative splicing of pyruvate kinase mRNA. Cancer Res. *70*, 8977–8980.

12. Zhang, Y., Li, J., Kong, L., Gao, G., Liu, Q.R., and Wei, L. (2007). NATsDB: Natural Antisense Transcripts DataBase. Nucleic Acids Res. *35*, D156–D161.

13. Lapidot, M., and Pilpel, Y. (2006). Genome-wide natural antisense transcription: coupling its regulation to its different regulatory mechanisms. EMBO Rep. *7*, 1216–1222.

14. Katayama, S., Tomaru, Y., Kasukawa, T., Waki, K., Nakanishi, M., Nakamura, M., Nishida, H., Yap, C.C., Suzuki, M., Kawai, J., et al.; RIKEN Genome Exploration Research Group; Genome Science Group (Genome Network Project Core Group); FANTOM Consortium (2005). Antisense transcription in the mammalian transcriptome. Science *309*, 1564–1566.

15. Khorkova, O., Myers, A.J., Hsiao, J., and Wahlestedt, C. (2014). Natural antisense transcripts. Hum. Mol. Genet. *23* (*Suppl R1*), R54–R63.

16. Villegas, V.E., and Zaphiropoulos, P.G. (2015). Neighboring gene regulation by antisense long non-coding RNAs. Int. J. Mol. Sci. *16*, 3251–3266.

17. Malhotra, S., Freeberg, M.A., Winans, S.J., Taylor, J., and Beemon, K.L. (2017). A Novel Long Non-Coding RNA in the hTERT Promoter Region Regulates hTERT Expression. Noncoding RNA *4*, 1.

18. Wang, Q., Zhang, J., Liu, Y., Zhang, W., Zhou, J., Duan, R., Pu, P., Kang, C., and Han, L. (2016). A novel cell cycle-associated lncRNA, HOXA11-AS, is transcribed from the 5-prime end of the HOXA transcript and is a biomarker of progression in glioma. Cancer Lett. *373*, 251–259.

19. Lv, Q.L., Hu, L., Chen, S.H., Sun, B., Fu, M.L., Qin, C.Z., Qu, Q., Wang, G.H., He, C.J., and Zhou, H.H. (2016). A Long Noncoding RNA ZEB1-AS1 Promotes Tumorigenesis and Predicts Poor Prognosis in Glioma. Int. J. Mol. Sci. *17*, 14.

20. Mineo, M., Ricklefs, F., Rooj, A.K., Lyons, S.M., Ivanov, P., Ansari, K.I., Nakano, I., Chiocca, E.A., Godlewski, J., and Bronisz, A. (2016). The Long Non-coding RNA HIF1A-AS2 Facilitates the Maintenance of Mesenchymal Glioblastoma Stem-like Cells in Hypoxic Niches. Cell Rep. *15*, 2500–2509.

21. Zhang, R., Jin, H., and Lou, F. (2018). The Long Non-Coding RNA TP73-AS1 Interacted With miR-142 to Modulate Brain Glioma Growth Through HMGB1/RAGE Pathway. J. Cell. Biochem. *119*, 3007–3016.

22. Xu, G., Liu, C., Li, G., Yu, Z., Wu, M. New exosomal long intergenic non-coding RNA (lncRNA) PRKAG2 antisense RNA 1 (PRKAG2-AS1), used for early diagnosis or prognosis of glioma. Patent CN103966337 A, filed May 26, 2014, and granted August 6, 2014.

23. Van Meir, E.G., Hadjipanayis, C.G., Norden, A.D., Shu, H.K., Wen, P.Y., and Olson, J.J. (2010). Exciting new advances in neuro-oncology: the avenue to a cure for malignant glioma. CA Cancer J. Clin. *60*, 166–193.

24. Fontana, L., Rovina, D., Novielli, C., Maffioli, E., Tedeschi, G., Magnani, I., and Larizza, L. (2015). Suggestive evidence on the involvement of polypyrimidine-tract binding protein in regulating alternative splicing of MAP/microtubule affinity-regulating kinase 4 in glioma. Cancer Lett. *359*, 87–96.

25. Xue, Y., Ouyang, K., Huang, J., Zhou, Y., Ouyang, H., Li, H., Wang, G., Wu, Q., Wei, C., Bi, Y., et al. (2013). Direct conversion of fibroblasts to neurons by reprogramming PTB-regulated microRNA circuits. Cell *152*, 82–96.

26. Lages, E., Guttin, A., El Atifi, M., Ramus, C., Ipas, H., Dupré, I., Rolland, D., Salon, C., Godfraind, C., deFraipont, F., et al. (2011). MicroRNA and target protein patterns reveal physiopathological features of glioma subtypes. PLoS ONE *6*, e20600.

27. Engels, B., Jannot, G., Remenyi, J., Simard, M.J., and Hutvagner, G. (2012). Polypyrimidine tract binding protein (hnRNP I) is possibly a conserved modulator of miRNA-mediated gene regulation. PLoS ONE *7*, e33144.

28. Li, C.L., Yang, W.Z., Chen, Y.P., and Yuan, H.S. (2008). Structural and functional insights into human Tudor-SN, a key component linking RNA interference and editing. Nucleic Acids Res. *36*, 3579–3589.

29. Paukku, K., Kalkkinen, N., Silvennoinen, O., Kontula, K.K., and Lehtonen, J.Y. (2008). p100 increases AT1R expression through interaction with AT1R 3′-UTR. Nucleic Acids Res. *36*, 4474–4487.

30. Cheung, H.C., Hai, T., Zhu, W., Baggerly, K.A., Tsavachidis, S., Krahe, R., and Cote, G.J. (2009). Splicing factors PTBP1 and PTBP2 promote proliferation and migration of glioma cell lines. Brain *132*, 2277–2288.

31. Coutinho-Mansfield, G.C., Xue, Y., Zhang, Y., and Fu, X.D. (2007). PTB/nPTB switch: a post-transcriptional mechanism for programming neuronal differentiation. Genes Dev. *21*, 1573–1577.

32. Hermansen, S.K., and Kristensen, B.W. (2013). MicroRNA biomarkers in glioblastoma. J. Neurooncol. *114*, 13–23.

33. Taniguchi, K., Sugito, N., Kumazaki, M., Shinohara, H., Yamada, N., Nakagawa, Y., Ito, Y., Otsuki, Y., Uno, B., Uchiyama, K., and Akao, Y. (2015). MicroRNA-124 inhibits cancer cell growth through PTB1/PKM1/PKM2 feedback cascade in colorectal cancer. Cancer Lett. *363*, 17–27.

34. Lin, N., Chang, K.Y., Li, Z., Gates, K., Rana, Z.A., Dang, J., Zhang, D., Han, T., Yang, C.S., Cunningham, T.J., et al. (2014). An evolutionarily conserved long noncoding RNA TUNA controls pluripotency and neural lineage commitment. Mol. Cell *53*, 1005–1019.

35. Ramos, A.D., Andersen, R.E., Liu, S.J., Nowakowski, T.J., Hong, S.J., Gertz, C., Salinas, R.D., Zarabi, H., Kriegstein, A.R., and Lim, D.A. (2015). The long noncoding RNA Pnky regulates neuronal differentiation of embryonic and postnatal neural stem cells. Cell Stem Cell *16*, 439–447.

36. Span, P.N., Rao, J.U., Oude Ophuis, S.B., Lenders, J.W., Sweep, F.C., Wesseling, P., Kusters, B., van Nederveen, F.H., de Krijger, R.R., Hermus, A.R., and Timmers, H.J. (2011). Overexpression of the natural antisense hypoxia-inducible factor-1alpha transcript is associated with malignant pheochromocytoma/paraganglioma. Endocr. Relat. Cancer *18*, 323–331.

37. Faghihi, M.A., Modarresi, F., Khalil, A.M., Wood, D.E., Sahagan, B.G., Morgan, T.E., Finch, C.E., St Laurent, G., III, Kenny, P.J., and Wahlestedt, C. (2008). Expression of a noncoding RNA is elevated in Alzheimer's disease and drives rapid feed-forward regulation of bold beta-secretase. Nat. Med. *14*, 723–730.

38. Su, W.Y., Li, J.T., Cui, Y., Hong, J., Du, W., Wang, Y.C., Lin, Y.W., Xiong, H., Wang, J.L., Kong, X., et al. (2012). Bidirectional regulation between WDR83 and its natural antisense transcript DHPS in gastric cancer. Cell Res. *22*, 1374–1389.

39. Qin, X., Yao, J., Geng, P., Fu, X., Xue, J., and Zhang, Z. (2014). LncRNA TSLC1-AS1 is a novel tumor suppressor in glioma. Int. J. Clin. Exp. Pathol. *7*, 3065–3072.

40. Carninci, P., Kasukawa, T., Katayama, S., Gough, J., Frith, M.C., Maeda, N., Oyama, R., Ravasi, T., Lenhard, B., Wells, C., et al.; FANTOM Consortium; RIKEN Genome Exploration Research Group and Genome Science Group (Genome Network Project Core Group) (2005). The transcriptional landscape of the mammalian genome. Science *309*, 1559–1563.

41. Wight, M., and Werner, A. (2013). The functions of natural antisense transcripts. Essays Biochem. *54*, 91–101.

42. Tan, X., Wang, S., Yang, B., Zhu, L., Yin, B., Chao, T., Zhao, J., Yuan, J., Qiang, B., and Peng, X. (2012). The CREB-miR-9 negative feedback minicircuitry coordinates the migration and proliferation of glioma cells. PLoS ONE *7*, e49570.

43. Munoz, J.L., Rodriguez-Cruz, V., and Rameshwar, P. (2015). High expression of miR-9 in $CD133^{+}$ glioblastoma cells in chemoresistance to temozolomide. J. Cancer Stem Cell Res. *3*, e1003.

44. Munoz, J.L., Rodriguez-Cruz, V., Walker, N.D., Greco, S.J., and Rameshwar, P. (2015). Temozolomide resistance and tumor recurrence: Halting the Hedgehog. Cancer Cell Microenviron. *2*, e747.

45. Faghihi, M.A., and Wahlestedt, C. (2009). Regulatory roles of natural antisense transcripts. Nat. Rev. Mol. Cell Biol. *10*, 637–643.

46. Leverson, J.D., Koskinen, P.J., Orrico, F.C., Rainio, E.M., Jalkanen, K.J., Dash, A.B., Eisenman, R.N., and Ness, S.A. (1998). Pim-1 kinase and p100 cooperate to enhance c-Myb activity. Mol. Cell *2*, 417–425.

47. Shaw, N., Zhao, M., Cheng, C., Xu, H., Saarikettu, J., Li, Y., Da, Y., Yao, Z., Silvennoinen, O., Yang, J., et al. (2007). The multifunctional human p100 protein 'hooks' methylated ligands. Nat. Struct. Mol. Biol. *14*, 779–784.

48. Cappellari, M., Bielli, P., Paronetto, M.P., Ciccosanti, F., Fimia, G.M., Saarikettu, J., Silvennoinen, O., and Sette, C. (2014). The transcriptional co-activator SND1 is a novel regulator of alternative splicing in prostate cancer cells. Oncogene *33*, 3794–3802.

49. Ponting, C.P. (1997). P100, a transcriptional coactivator, is a human homologue of staphylococcal nuclease. Protein Sci. *6*, 459–463.

50. Li, C.H., and Chen, Y. (2013). Targeting long non-coding RNAs in cancers: progress and prospects. Int. J. Biochem. Cell Biol. *45*, 1895–1910.

51. Wahlestedt, C. (2006). Natural antisense and noncoding RNA transcripts as potential drug targets. Drug Discov. Today *11*, 503–508.

52. Khorkova, O., Hsiao, J., and Wahlestedt, C. (2015). Basic biology and therapeutic implications of lncRNA. Adv. Drug Deliv. Rev. *87*, 15–24.

53. Quinn, J.J., and Chang, H.Y. (2016). Unique features of long non-coding RNA biogenesis and function. Nat. Rev. Genet. *17*, 47–62.

54. Huarte, M. (2015). The emerging role of lncRNAs in cancer. Nat. Med. *21*, 1253–1261.

YMTHE, Volume *27*

Supplemental Information

PTB-AS, a Novel Natural Antisense Transcript, Promotes Glioma Progression by Improving PTBP1 mRNA Stability with SND1

Liyuan Zhu, Qunfang Wei, Yingjiao Qi, Xiangbin Ruan, Fan Wu, Liang Li, Junjie Zhou, Wei Liu, Tao Jiang, Jing Zhang, Bin Yin, Jiangang Yuan, Boqin Qiang, Wei Han, and Xiaozhong Peng

Supplemental Figures and Figure Legends

Figure S1

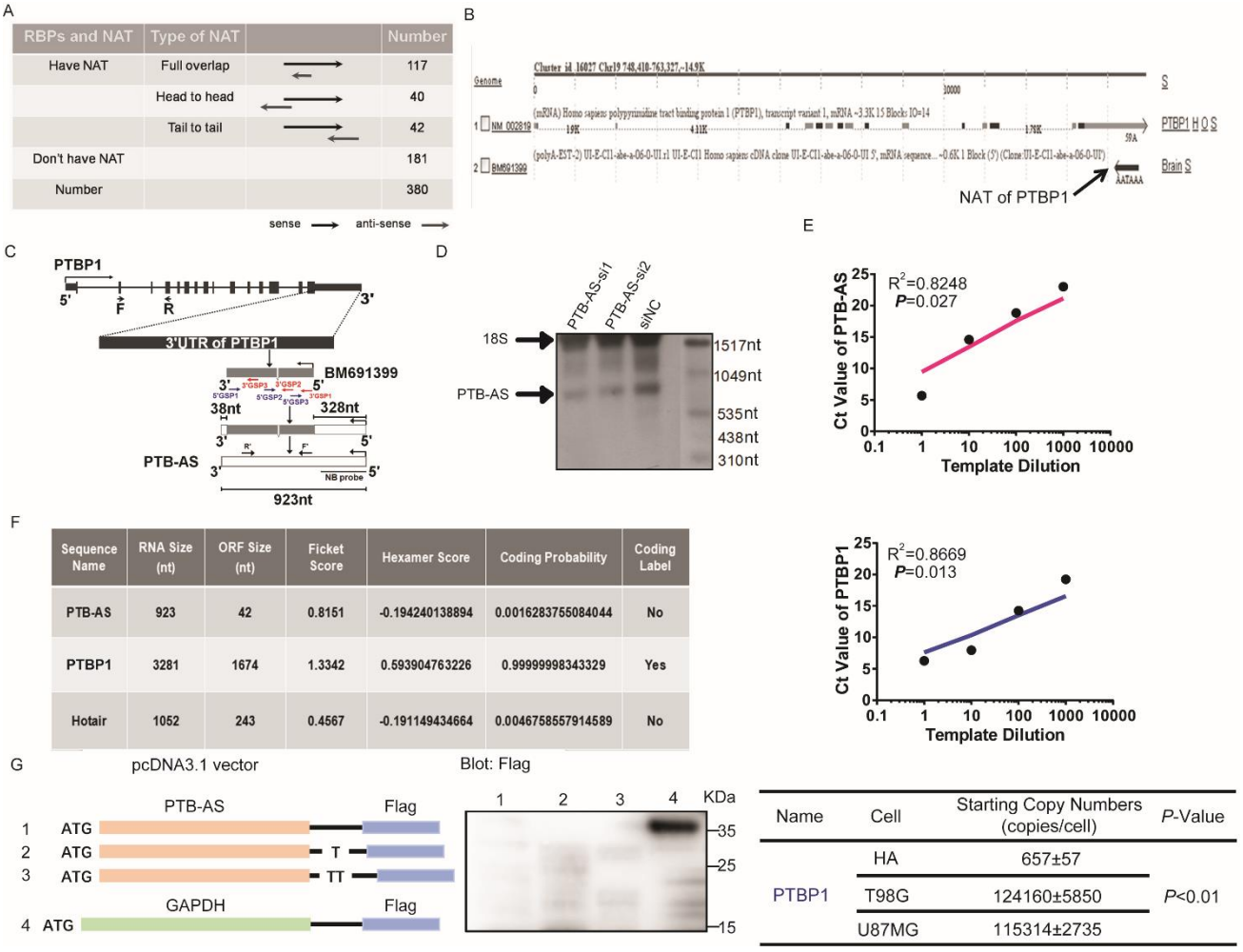

Suppl Figure S1: The overview of screening results for RBPs associated NATs and identification of PTBP1 NAT.

A. The statistics of the screening results for RBPs and the subtype of the NATs.

B. NAT of PTBP1 was located in the 3'UTR of PTBP1 and owns the poly (A) tail. The black stick which had been directed by arrow indicated the NAT of PTBP1.

C. U87MG cell was transfected with PTB-AS-siRNA or siNC and the total RNA was extracted for northern blot. The amount of total RNA each lane was equivalent. The sharp band directed by the subjacent arrow was PTB-AS.

D. The relative genomic locus of PTB-AS and PTBP1. The raw transcript of PTB-AS, BM691399, was totally overlapped by PTBP1-3'UTR. By using 5'& 3' RACE, the full length of PTB-AS was identified as 923nt. NB probe indicated the real position of probe for Northern Blot.

E. The starting copy number was detected and calculated to quantify the expression of PTBP1 in HA, T98G or U87MG cell lines using absolute Quantification PCR. The standard curve was made according to the starting cycle value of PTB-AS and PTBP1, respectively.

F. Coding potential prediction for PTB-AS using CPC and CPAT software. PTBP1 and HOTAIR acted as coding and non-coding transcript positive controls, respectively.

G. Full-length PTB-AS was cloned into pcDNA3.1 (with N-terminal start codon ATG and C-terminal Flag tag) in all three coding patterns and subsequently transfected into HEK293T cells separately. GAPDH (the mRNA length was close to PTB-AS) with Flag tag severs as a positive control. Western blot was performed to detect the Flag-tagged protein after 48 hours. Data are representative of three independent experiments.

Figure S2

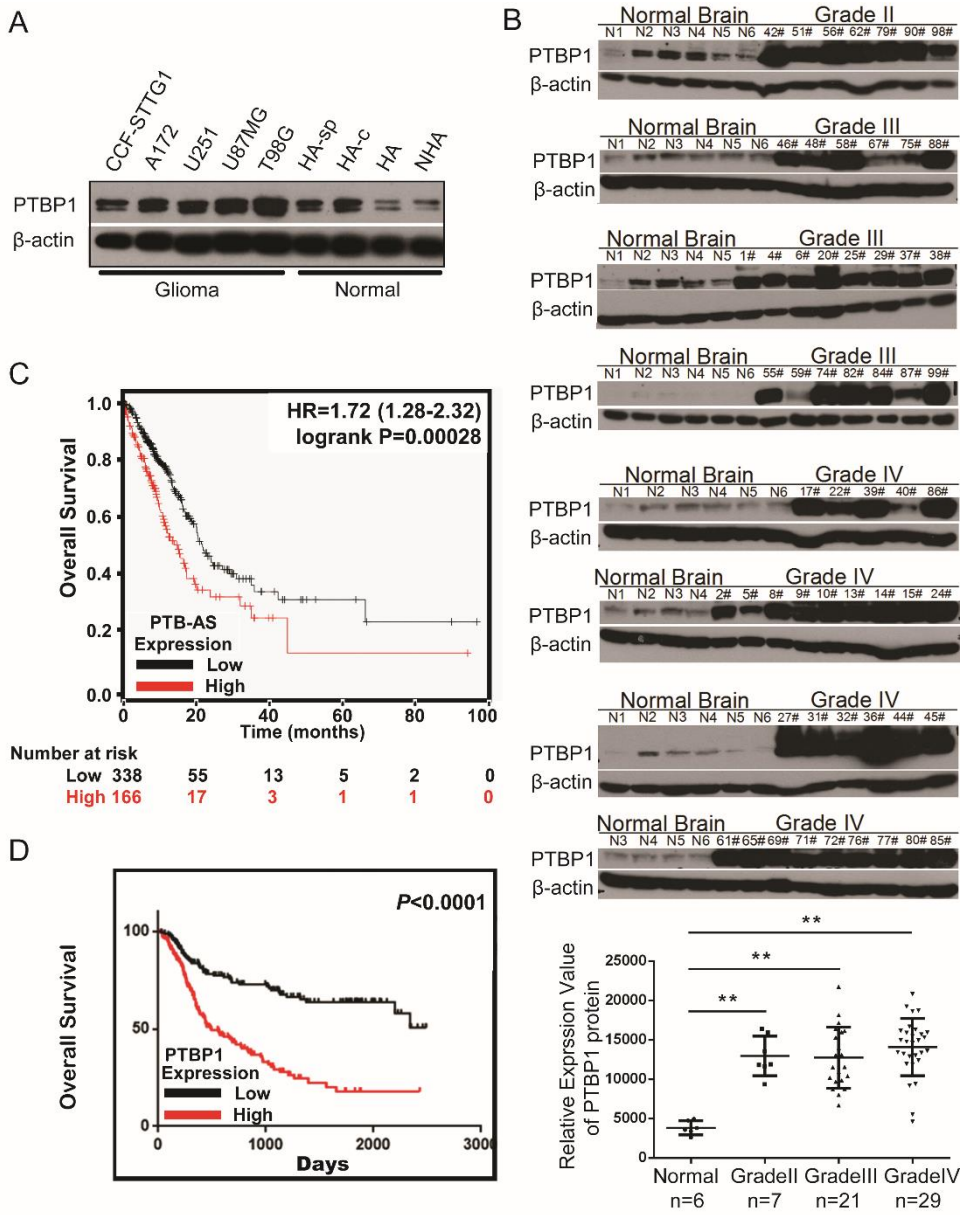

Suppl Figure S2: The raw data of PTBP1 which expressed and functioned in glioma.

A. Western blotting result showed the expression level of PTBP1 protein in 5 glioma cell lines and 4 human astrocyte cell lines.

B. Relative expression level of PTBP1 protein in 6 control brain tissues, representative 7 grade II, 21 grade III, and 29 grade IV glioma tissues by western blotting (β-actin was used as the internal parameters) and analysis the value of grey scale scanning the corresponding bands after western blotting. The protein expression levels of PTBP1 are relatively expressed as the mean ± SD, n = 3. *P< 0.05; **P<0.01 (Student's t test).

C. The Kaplan–Meier curve analysis on the impact of PTB-AS expression on overall survival. P value was calculated by Log Rank test.

D. The differential overall survival curve of high or low PTBP1 expressed patients. Kaplan–Meier curve analysis on the impact of PTBP1 expression. P value was calculated by Log Rank test.

Figure S3

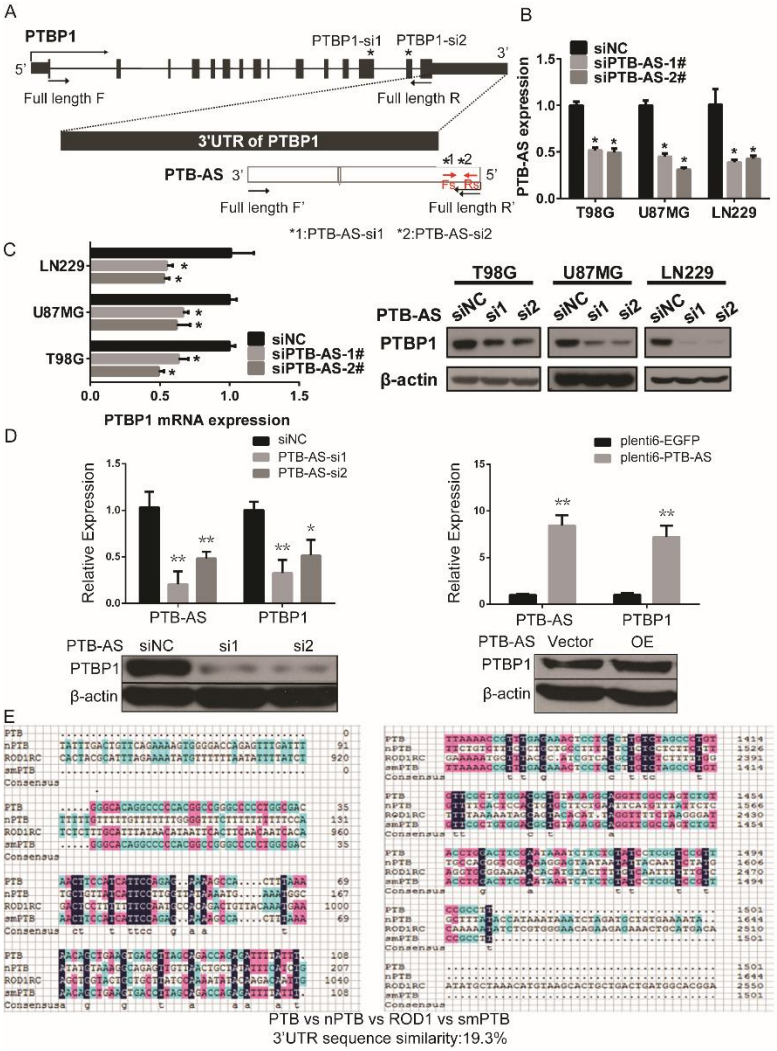

Suppl Figure S3: The target site of stealth siRNAs of PTB-AS and PTBP1.

A. The detail graph which shown the target site (marked *) of stealth siRNAs of PTB-AS and PTBP1, as well as the position of primers (Full length F&R, F'&R') for PTB-AS or PTBP1 overexpression. The specific primers Fs&Rs of PTB-AS were used for qRT-PCR. The target of siRNAs for PTB-AS located in the non-overlapped area with PTBP1-3'UTR in order to avoid off-target effect.

B&C. Changes in PTB-AS level alter PTBP1 mRNA and protein levels. T98G, U87MG or LN229 cells were infected with two different siRNAs (PTB-AS si1 or PTB-AS si2) to knock down. PTB-AS (using Fs&Rs primer pair) and PTBP1 mRNA level were measured by qRT-PCR. PTBP1 protein level was measured by western blot. n=3. *P<0.05 (Student's t test).

D. A172 cells were transfected with two different PTB-AS siRNAs, siNC or PTB-AS-plenti6 plasmid, plenti6-EGFP, separately. Then total RNA of differential treatment cells was extracted for reverse transcription. Following qRT-PCR and western blotting were performed to test the expression changes of PTBP1 in RNA and protein level after knocking down PTB-AS. The expression of PTBP1 in RNA level is relatively showed as the mean ± SD, n = 3. *P< 0.05; **P<0.01 (Student's t test).

E. Alignment of 3'UTR of PTBP1 family members using DNAman. The bases in dark blue indicated the absolutely similar sequence of the four members, the pink one indicated three members had this base in the same position, and the light green one indicated that only two members share the same base.

Figure S4

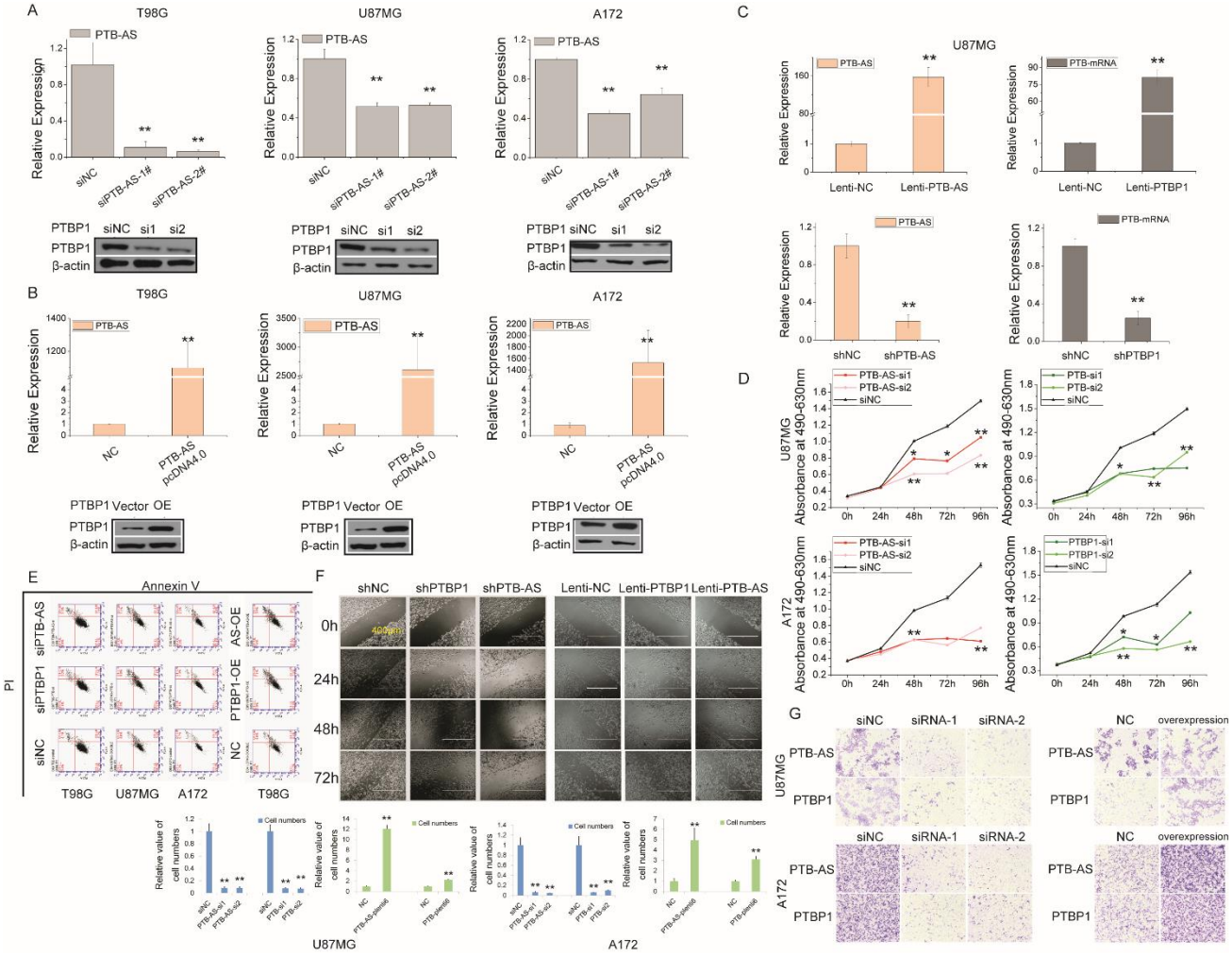

Suppl Figure S4: The biological function of PTB-AS and PTBP1 in glioma

A, B and C. Quantitative real-time PCR and western blotting were performed to identify the efficiency of PTB-AS and PTBP1 knocking down or overexpressing in T98G, U87MG and A172 glioma cell lines. The RNA levels of PTB-AS and PTBP1 are relatively expressed as the mean ± SD, n = 3. *P< 0.05; **P<0.01; ***P<0.001 (Student's t test).

D. MTS assays shown the growth curve of U87MG and A172 cell lines after transfecting siRNAs against PTB-AS or PTBP1, following individually test the absorbance in 490nm and 630nm. Results are expressed as mean ± SD, n = 4. *P < 0.05; **P < 0.01 (Student's t test).

E. Annexin V-FITC and PI co-staining to identify the apoptosis of glioma cells (T98G, U87MG and A172) after transfected with the knocking down or overexpressing materials of PTB-AS or PTBP1, respectively.

F. The wound-healing images, which represents the relative area of the remaining open wound calculated in relation to that at time 0 h after PTB-AS/PTBP1 knockdown or overexpression.

G. Transwell migration assays of U87MG and A172 glioma cell line transfected with siRNAs or plasmids for PTB-AS and PTBP1 knocking down or overexpressing, respectively. Fixation and staining were performed after transfection for 72h. The results are representative of at least three independent experiments. Graphs indicate the average number of cells per field of the indicated cell lines in migration assays. Results show the mean ± SD, *P<0.05, **P<0.01 (Student's t test).

Figure S5

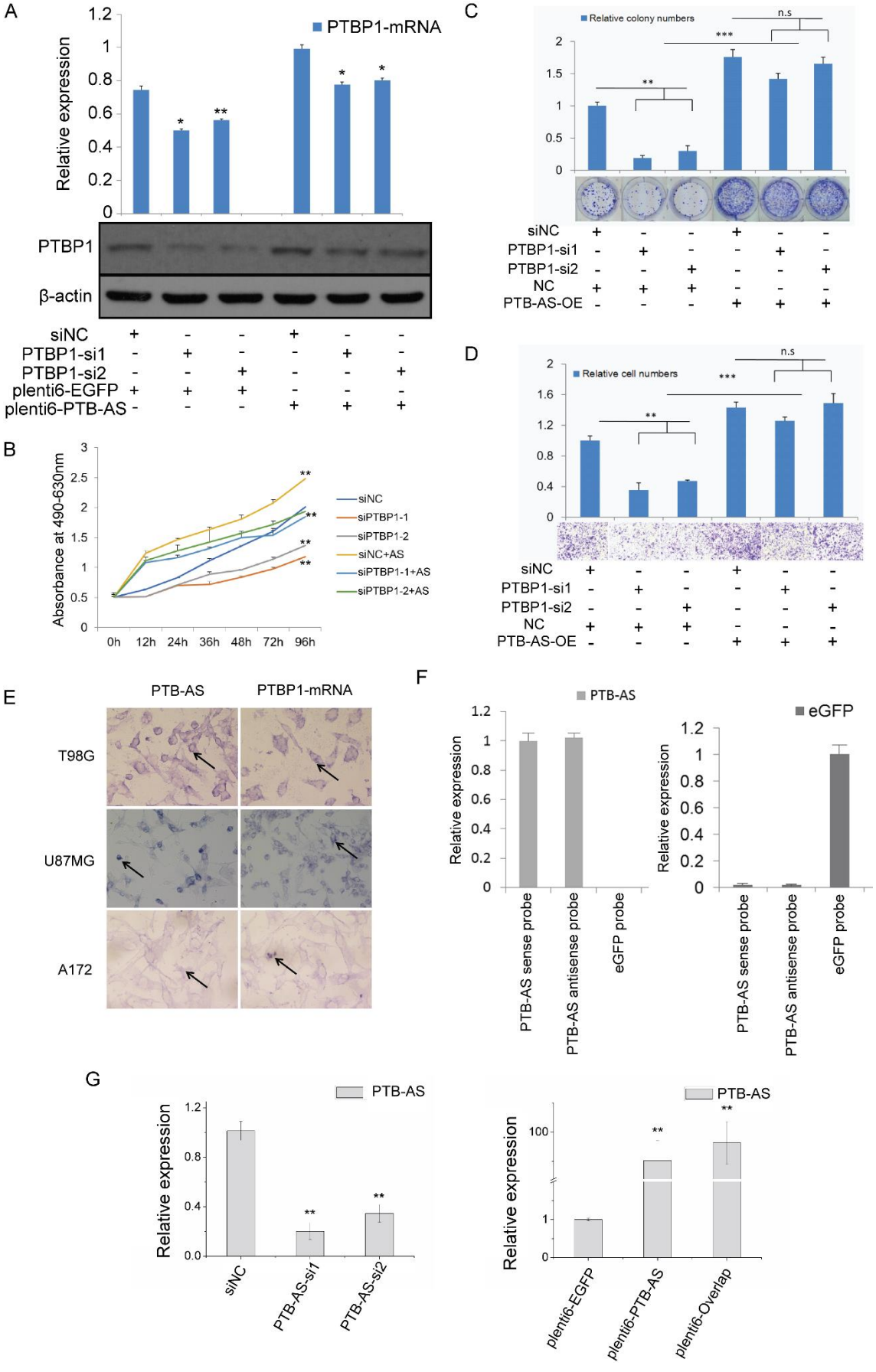
A
PTBP1-mRNA
Relative expression
PTBP1
β-actin
siNC
PTBP1-si1
PTBP1-si2
plenti6-EGFP
plenti6-PTB-AS
B
Absorbance at 490-630nm
0h 12h 24h 36h 48h 72h 96h
siNC
siPTBP1-1
siPTBP1-2
siNC+AS
siPTBP1-1+AS
siPTBP1-2+AS
C
Relative colony numbers
n.s
siNC
PTBP1-si1
PTBP1-si2
NC
PTB-AS-OE
D
Relative cell numbers
n.s
siNC
PTBP1-si1
PTBP1-si2
NC
PTB-AS-OE
E
PTB-AS
PTBP1-mRNA
T98G
U87MG
A172
F
PTB-AS
eGFP
Relative expression
PTB-AS sense probe
PTB-AS antisense probe
eGFP probe
G
PTB-AS
Relative expression
siNC
PTB-AS-si1
PTB-AS-si2
plenti6-EGFP
plenti6-PTB-AS
plenti6-Overlap

Suppl Figure S5: PTB-AS could rescue the down regulation of PTBP1 through binding to PTBP1-3'UTR in cytoplasm and influenced PTBP1 mRNA stability.

A. The glioma cell U87MG was co-transfected with PTBP1-siRNA and PTB-AS-OE (plenti6-PTB-AS) in order to perform the rescue experiment. SiNC or NC (plenti6-EGFP), as the negative control, was used to make permutation and combination with PTBP1-siRNA or PTB-AS-OE. Following qRT-PCR and western blotting were operated to test the expression changes of PTBP1 in RNA and protein level. The expression of PTBP1 in RNA level is relatively showed as the mean ± SD, n = 3. **P*< 0.05; ***P*<0.01 (Student's t test).

B, C and D. The glioma cell U87MG was co-transfected with PTBP1-siRNA and PTB-AS-OE (plenti6-PTB-AS) in order to perform the rescue experiment. SiNC or NC (plenti6-EGFP), as the negative control, was used to make permutation and combination with PTBP1-siRNA or PTB-AS-OE. Following MTS assays (B), colony formation (C) and transwell migration assays (D) were performed to identify the rescue effect of PTB-AS to PTBP1 in regulating glioma tumorigenesis. Graphs indicate the average number of cells per field of the indicated cell lines in migration assays. The cell colonies were counted by Image-Pro Plus software and plotted. Data were expressed as mean ± SD, n = 5. **P* < 0.05; ***P* < 0.01 (Student's t test).

E. In situ hybridization for PTB-AS and PTBP1 on slides through T98G, U87MG and A172 cell. All images show the same magnification (40X). PTB-AS and PTBP1-mRNA intracellular localization was visualized in cytoplasm as the arrows directed.

F. U87MG cell were transfected with biotinylated the full length of PTB-AS or biotinylated eGFP as the NC. PTB-AS and eGFP expression levels were analysed by qRT-PCR. Data were expressed as mean ± SD, n = 3.

G. The identification of effect on PTB-AS knocking down or overexpression before half-life assay. QRT-PCR was used to show the expression of PTB-AS. Data are shown as mean ±SD of three independent experiments. ***P*<0.01(Student's t test).

Figure S6

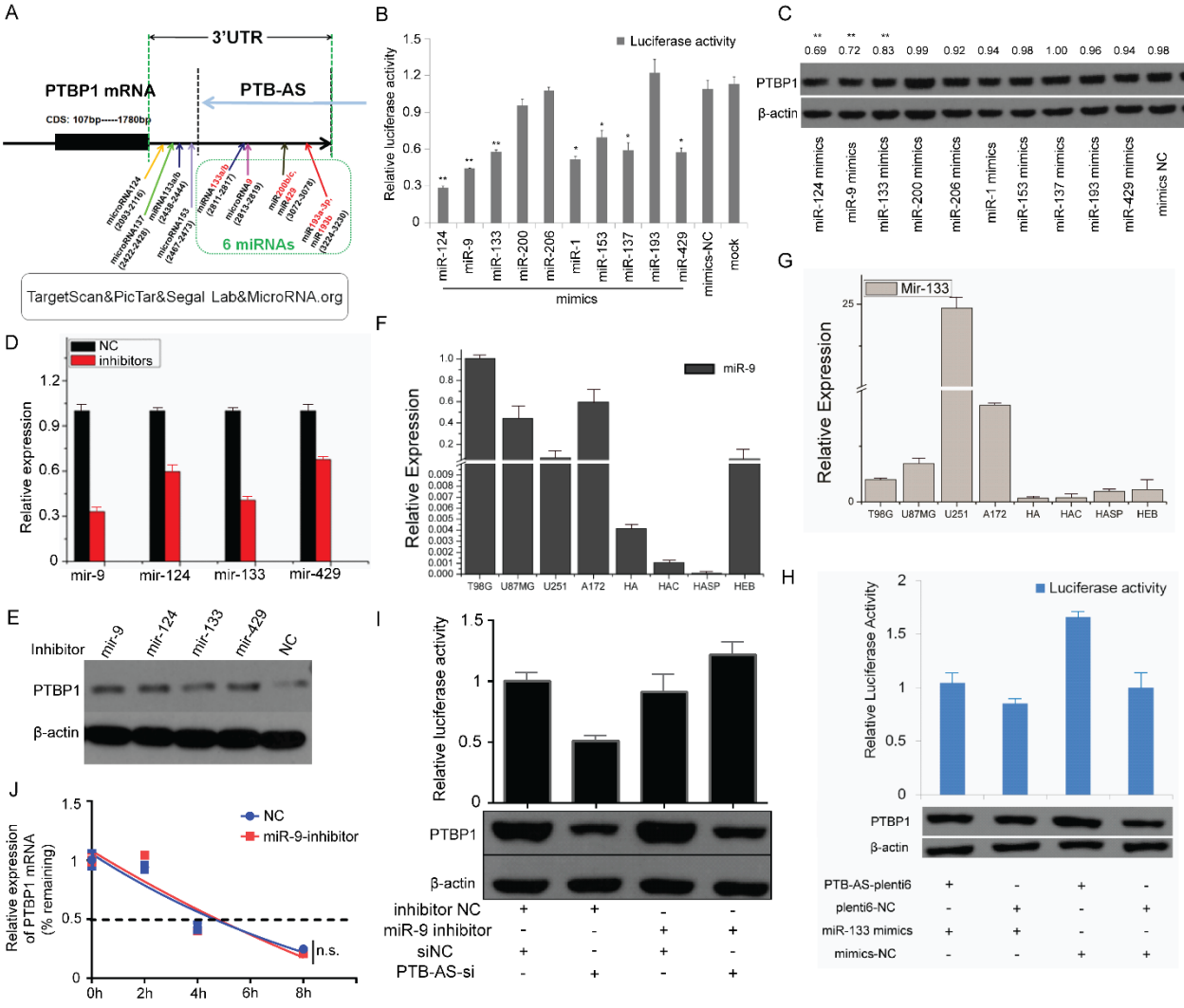

Suppl Figure S6: MiR-9 plays significant role in regulating PTBP1 expression.

A. Potential miRNAs which regulated PTBP1 were predicted using integrated bioinformatics tools and the relative position of binding site for these miRNAs.

B. All of miRNA mimics were separately transfected in U87MG cells and luciferase reporter assays were performed. Relative luciferase activity value was shown as the mean ± SD, n=3. *P<0.05, **P<0.01 (t test).

C. Western blotting experiments were performed after transfection of the mimics. The results of western blotting were quantified by densitometry and are shown as the ratios of PTBP1/β-actin protein levels (the values shown above the blots). Results were from three biological replicates.

D and E. U87MG were transfected with potential miRNAs to identify the effect of miRNAs on expression of PTBP1. Quantitive real-time PCR were performed to validate the changing of miRNAs. Data were expressed as mean ± SD, n = 3. Western blotting experiments were performed to identify the effect of miRNAs inhibitors on expression of PTBP1.

F and G. Relative expression profile of miR-9 or miR-133 in glioma and normal astrocyte cells. Quantitative real-time PCR was performed. Data were expressed as mean ± SD, n = 3.

H. Luciferase reporter assays and western blotting experiments were performed to validate the miR-

133 misregulated PTBP1 caused by overexpression of PTB-AS. Data were expressed as mean ± SD, n = 3. Relative luciferase activity value was shown as the best result of two replicates. The results of western blotting were from three biological replicates.

I. U87MG cell were co-transfected with miR-9 inhibitor and PTB-AS-siRNA, and siNC or inhibitor-NC were negative control. Luciferase reporter assays and western blotting experiments were performed to validate the miR-9 re-regulated PTBP1 caused by downregulation of PTB-AS. Data were expressed as mean ± SD, n = 3. Relative luciferase activity value was shown as the best result of two replicates. The results of western blotting were from three biological replicates.

J. Half-life assay for PTBP1 mRNA after inhibiting miR-9 expression. NC or miR-9 inhibitor was transfected into U87MG cells. Transcript decay curves were measured after transfection for 48 h when transcription was blocked by adding actinomycin D (5 μg/mL). Transcripts remaining relative to the control gene were assessed by qRT-PCR. N.S. indicates no significance, and the analyses used nonlinear regression (one phase decay curve fit) to determine the half-life. Error bars show the standard deviation. The results were from three biological replicates.

Figure S7

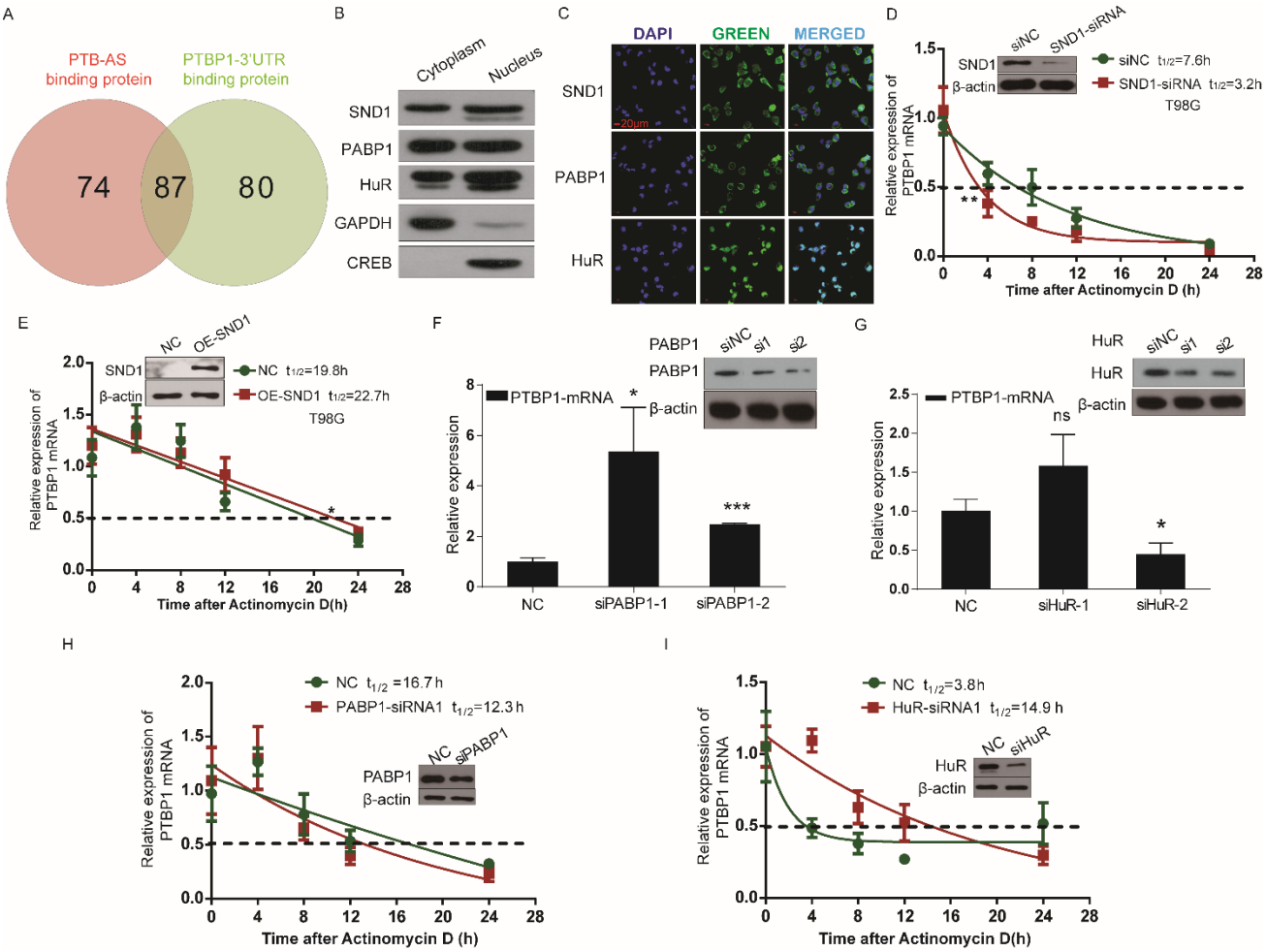

Suppl Figure S7: Effects of HuR and PABP1 in the expression and half-life of PTBP1 mRNA.

A. Venn diagram showing the overlap of genes occupied by genes pulled down by PTB-AS probe and PTBP1-3'UTR probe at high confidence in T98G cells as determined by mass spectrometry.

B&C. The cytoplasm/nuclear separation experiment and immunofluorescence (IFC) assay show the cellular localization of candidate proteins in glioma cells. GAPDH and CREB act as the positive control indicating cytoplasm or nuclear compositions, respectively. Scale Bar: 20 μ m.

C and D. T98G cells expressing control siRNA or SND1 siRNA / mock-vector (NC) or pcDNA4.0-SND1 plasmid (OE-SND1) were treated with actinomycin D (5 μg/mL) for the indicated periods of time. Total RNA was then analysed by RT-qPCR to examine the mRNA half-life of PTBP1. Half-life was calculated by using one phase decay; Data shown are the mean ± SD (n = 3; **P*<0.05, ***P*<0.01, two-tailed t-test).

E and F. T98G cells were infected with two different siRNAs ((A) PABP1-siRNA1 or PABP1-siRNA2 and (B) HuR-siRNA1 or HuR-siRNA2) to knock down each gene. PTBP1 mRNA level were calculated by RT-qPCR. Data were expressed as mean ± SD, n = 3. **P* < 0.05; ***P* < 0.01, ****P* < 0.001 (Student's t test).

G and H. T98G cells expressing target or control siRNAs were treated with actinomycin D (5 μg/mL) for the indicated periods of time. Total RNA was then analyzed by RT-qPCR to examine the half-life of PTBP1 mRNA. Half-life was calculated with linear fitting. Data were expressed as mean ± SD, n = 3. **P* < 0.05; ***P* < 0.01, ****P*<0.001 (Student's t test).

Supplemental Tables and Table Legends

Supplemental Table S1: List of 380 genes identified as putative RBPs.

RBPs Names	Domain	ISH Profiled?
Fxr2	KH	x
Tdrkh	KH	x
Retrovirus-related gag	other	x
gene model 381	KH	
similar to HPRP18	other, prp18	x
Bicc1	KH	x
cw17	KH	x
Fmr1	KH	x
Refbp1	RRM	x
Cpsf1	RRM	x
Daz1	RRM	x
Elavl3	RRM	x
Ewsh	RRM	x
Nssr	RRM	x
G3bp1	RRM	x
Nsap11	RRM	x
Hnrpa/b	RRM	x
Pabpc4l	RRM	x
Pparg1b	RRM	x

Ptbp2	**RRM**	**x**
Rbmy1a1	**RRM**	**x**
4921506I22Rik	**RRM**	**x**
Msi1h	**RRM**	**x**
Silg41	**RRM**	**x**
Rbpms2	**RRM**	**x**
3000004N20Rik	**RRM**	**x**
5730555F13Rik	**RRM**	**x**
2810036L13Rik	**RRM**	**x**
2610101N10Rik	**RRM**	**x**
8030431D03Rik	**RRM**	**x**
4932702K14Rik	**RRM**	**x**
U2af1	**RRM**	**x**
1700012H05Rik	**RRM**	**x**
Snrpb2	**RRM**	**x**
Rbm28	**RRM**	**x**
Snrp70	**RRM**	**x**
6330548G22Rik	**RRM**	**x**
C330027G06Rik	**RRM**	**x**
Rbm18	**RRM**	**x**
2610019N13Rik	**RRM**	**x**
2610020H08Rik	**RRM**	**x**
Rad52b	**RRM**	**x**
2610015J01Rik	**RRM**	**x**

Rdbp	**RRM**	**x**
Drbp1	**RRM**	**x**
Refbp2	**RRM**	**x**
Sfrs4	**RRM**	**x**
Ppargc1	**RRM**	**x**
4930565A21Rik	**RRM**	**x**
U2af2	**RRM**	**x**
LOC381370	**RRM**	**x**
LOC225307	**RRM**	**x**
2310016K04Rik	**dsRM**	**x**
Tarbp2	**dsRM**	**x**
Spnr	**dsRM**	**x**
Adar3	**dsRM**	**x**
Tenr	**dsRM**	**x**
Mrlp44	**dsRM**	**x**
Dhx30	**dsRM**	**x**
2810055E05Rik	**other, S1**	**x**
2610029K21Rik	**G-patch**	**x**
2010009L17Rik	**G-patch**	**x**
1300018I05Rik	**G-patch**	**x**
Bat4	**G-patch**	**x**
Hrmt1l3	**other, arginine N-methyltransferase**	**x**
LOC381813	**other, arginine N-methyltransferase**	**x**
Hrmtl16	**other, arginine N-methyltransferase**	**x**

LOC215034	**Piwi**	**x**
Top3a	**Zinc Knuckle**	**x**
3110031B13Rik	**Zinc Knuckle**	**x**
BC005685	**other**	**x**
Cnbp2	**Zinc Knuckle**	**x**
Zcchc10	**Zinc Knuckle**	**x**
2700088M22Rik	**RRM**	**x**
1500031H04Rik	**Zinc Knuckle**	**x**
Zcchc4	**Zinc Knuckle**	**x**
Zcchc12	**Zinc Knuckle**	**x**
Rn7sk	**other**	**x**
2610524B01Rik	**other, PHD**	**x**
Rpo2tc1	**other, transcription**	**x**
LOC218298	**other, SKIP**	**x**
AI033314	**Tudor**	**x**
2410004F06Rik	**Tudor**	**x**
Gtrosa26as	**other, THUMP**	**x**
Adam5	**other, Zn dependent metaloproteinase domain**	**x**
Traf6	**RRM**	**x**
D3Wsu161c	**RRM**	**x**
Tlr5	**RRM**	**x**
0610009D07Rik	**RRM**	**x**
5430431G03Rik	**RRM**	**x**

2600016B03Rik	RRM	x
1810073H04Rik	RRM	x
0610033I05Rik	RRM	x
1110007F05Rik	RRM	x
2610024N24Rik	RRM	x
2010015M23Rik	RRM	x
1700009P03Rik	RRM	x
9530027K23Rik	RRM	x
Tdrd7	RRM	x
Rbm16	RRM	x
2610209F03Rik	RRM	x
V1rc17	RRM	x
2210008M09Rik	RRM	x
Pprc1	RRM	x
D8ertd233e	RRM	x
D330023I21Rik	RRM	x
A430091O22Rik	RRM	x
BC013481	RRM	x
5730453I16Rik	RRM	x
4921511I16Rik	dsRM	x
4930403J07Rik	dsRM	x
Snrpe	other, Sm protein	x
2810441A10Rik	other, U5 snRNP associated domain	x
2610031L17Rik	other, HAT	x

Snrpa1	**other, LRR**	**x**
Prpf3	**other, PWI**	**x**
Sf3a3	**other, PRP9**	**x**
Sf3b3	**other, CPSF**	**x**
Sf3b4	**RRM**	**x**
Nxf2	**other, TAP-C**	**x**
Nxf7	**other, TAP-C**	**x**
Eif4a1	**DEAD, Superfamily II RNA helicase**	**x**
Srrm1	**other, PWI**	**x**
Ddx39	**DEAD, Superfamily II RNA helicase**	**x**
G430041M01Rik	**RRM**	**x**
Lsm6	**other, Sm-protein**	**x**
LOC384385	**other, prp18**	**x**
MCG1038304	**RRM**	**x**
Ascc3l1	**DEAD, Superfamily II RNA helicase**	**x**
MCG1027004	**RRM**	**x**
BC035291	**RRM**	**x**
LOC216024	**RRM**	**x**
Rbm11	**RRM**	**x**
E030019O05	**RRM**	**x**
D11Bwg0517e	**RRM**	**x**
9930033H14Rik	**RRM**	**x**
1810017N16Rik	**RRM**	**x**
Gm761	**RRM**	**x**

1700128F08Rik	**RRM**	**x**
LOC436185	**RRM**	**x**
LOC195154	**RRM**	**x**
Gm411	**KH**	**x**
Gm1424	**KH**	**x**
Nova1	**KH**	**x**
Gm381	**KH**	**x**
1810003N24Rik	**KH**	**x**
Htatsf1	**RRM**	**x**
Cpeb4	**RRM**	**x**
LOC433054	**RRM**	
LOC237032	**RRM**	
Miwi	**Piwi**	
D8ertd233e	**RRM**	
Rbmx2	**RRM**	
MCG51890	**RRM**	
AA517739	**RRM**	
B230333C21Rik	**RRM**	
C330012H03Rik	**KH**	
C530047H08Rik	**RRM**	
Cstf2t	**RRM**	
Oog4	**KH**	
Rps3	**KH**	
1810035L17Rik	**RRM**	

ds8	**G-patch**	
Khsrp	**KH**	
Mela	**Zinc Knuckle**	
C430048L16Rik	**RRM**	
Cstf2	**RRM**	
Dppa5	**KH**	
Sfrs15	**RRM**	
Raver	**RRM**	
Rkhd1	**KH**	
Rkhd2	**KH**	
Rkhd3	**KH**	
1700025B16Rik	**RRM**	
2410104I19Rik	**RRM**	
2810441O16Rik	**RRM**	
3100004P22Rik	**RRM**	
4930562C03Rik	**RRM**	
4933434H11Rik	**RRM**	
6430512A10Rik	**RRM**	
Pcbp2	**KH**	**x**
Pcbp4	**KH**	**x**
Igf2bp1	**KH**	**x**
Fxr1	**KH**	**x**
Hnrpk	**KH**	**x**
Igf2bp3	**KH**	**x**

Khdrbs1	**KH**	**x**
Qk	**KH**	**x**
Khdrbs2	**KH**	**x**
Khdrbs3	**KH**	**x**
Ascc1	**KH**	**x**
Boll	**RRM**	**x**
Brunol4	**RRM**	**x**
Mint	**RRM**	**x**
Cpeb	**RRM**	**x**
Cugbp1	**RRM**	**x**
Elavl2	**RRM**	**x**
Elavl4	**RRM**	**x**
Cugbp2	**RRM**	**x**
G3bp2	**RRM**	**x**
Hnrpa1	**RRM**	**x**
Hnrpc	**RRM**	**x**
Hnrph1	**RRM**	**x**
Hnrph2	**RRM**	**x**
Hnrpr	**RRM**	**x**
Raly	**RRM**	**x**
Hnrpdl	**RRM**	**x**
Ssb	**RRM**	**x**
Myef2	**RRM**	**x**
Rbm4	**RRM**	**x**

Msi2h	**RRM**	**x**
Rbms1	**RRM**	**x**
Cnot4	**RRM**	**x**
Np220	**RRM**	**x**
Nsap1	**RRM**	**x**
Ncl	**RRM**	**x**
Pabpc2	**RRM**	**x**
Kist	**KH**	**x**
Fus	**RRM**	**x**
Pabpn1	**RRM**	**x**
Ptbp1	**RRM**	**x**
Sfpq	**RRM**	**x**
Rbm10	**RRM**	**x**
Rbm3	**RRM**	**x**
Rbm6	**RRM**	**x**
Rbmx	**RRM**	**x**
Rbpms	**RRM**	**x**
Rnps1	**RRM**	**x**
Sart3	**RRM**	**x**
Rbms2	**RRM**	**x**
Rnpc1	**RRM**	**x**
Sfrs10	**RRM**	**x**
Sfrs2	**RRM**	**x**
Snrpa	**RRM**	**x**

U2af1-rs1	**RRM**	**x**
U2af1-rs2	**RRM**	**x**
Synj2	**RRM**	**x**
Tia1	**RRM**	**x**
Tial1	**RRM**	**x**
Ppil4	**RRM**	**x**
Rbm19	**RRM**	**x**
Rbm8	**RRM**	**x**
Rbm22	**RRM**	**x**
Nono	**RRM**	**x**
Sfrs6	**RRM**	**x**
Sfrs9	**RRM**	**x**
Rbm14	**RRM**	**x**
Pabpc1	**RRM**	**x**
Pspc1	**RRM**	**x**
Hnrpm	**RRM**	**x**
Rbm12	**RRM**	**x**
Nol8	**RRM**	**x**
Tnrc6	**RRM**	**x**
Rnpc2	**RRM**	**x**
Acin1	**RRM**	**x**
A2bp1	**RRM**	**x**
Ppie	**RRM**	**x**
Cirbp	**RRM**	**x**

Stau2	**dsRM**	**x**
Stau1	**dsRM**	**x**
Prkra	**dsRM**	**x**
Ilf3	**dsRM**	**x**
Adarb1	**dsRM**	**x**
Adar	**dsRM**	**x**
Prkr	**dsRM**	**x**
Ddx9	**dsRM**	**x**
Pdcd11	**other, S1**	**x**
Supt6h	**other, S1**	**x**
Tfip11	**G-patch**	**x**
Rbm5	**G-patch**	**x**
Pum1	**other, PUF**	**x**
Hrmt1l2 (PRMT1)	**other, arginine N-methyltransferase**	**x**
Hrmt1l1	**other, arginine N-methyltransferase**	**x**
Piwil2	**Piwi**	**x**
Eif2c4	**Piwi**	**x**
Eif2c3	**Piwi**	**x**
Peg10	**Zinc Knuckle**	**x**
Cnbp	**other, arginine N-methyltransferase**	**x**
Zcchc7	**Zinc Knuckle**	**x**
Pnpt1	**KH**	**x**
Carm1	**other, arginine N-methyltransferase**	**x**
Cops5	**other, CSN5 domain**	**x**

Scand1	**other, LR**	**x**
Ncoa6ip	**other, THUMP**	**x**
Ncoa3	**other, PAS**	**x**
Ptcd2	**other, PPR**	**x**
Ptcd1	**other, PPR**	**x**
Akap1	**KH**	**x**
Sfrs1	**RRM**	**x**
Hnrpd	**RRM**	**x**
Son	**dsRM**	**x**
Eif2c2 (AGO2)	**Piwi**	**x**
Dazap1	**RRM**	**x**
Col4a3	**RRM**	**x**
Hnrpl	**RRM**	**x**
Htf9c	**RRM**	**x**
Rbmxrt	**RRM**	**x**
Rpo1-2	**RRM**	**x**
Eif3s9	**RRM**	**x**
Afg3l2	**RRM**	**x**
Rbm21	**RRM**	**x**
Poldip3	**RRM**	**x**
Rbm17	**RRM**	**x**
Wdr9	**RRM**	**x**
Slc6a8	**RRM**	**x**
Hnrpa3	**RRM**	**x**

Rbms3	**RRM**	**x**
Cova1	**RRM**	**x**
Rnpep	**RRM**	**x**
Safb	**RRM**	**x**
Rbm27	**RRM**	**x**
Tardbp	**RRM**	**x**
Grsf1	**RRM**	**x**
Rbed1	**RRM**	**x**
Csad	**RRM**	**x**
Lsm4	**other, Sm protein**	**x**
Lsm7	**other, Sm protein**	**x**
Crnkl1	**other, HAT**	**x**
Sf3a1	**other, SWAP**	**x**
Snrpg	**other, Sm protein**	**x**
Cpsf5	**other, mRNA cleavage factor**	**x**
Snrpf	**other, Sm protein**	**x**
Prp17	**other, WD40**	**x**
Sf3b1	**other, U2 snRNP spliceosome subunit**	**x**
Prpf8	**other, JAB/MPN**	**x**
Nxt1	**other, NTF2**	**x**
Nxf1	**other, TAP-C**	**x**
Rpl5	**other, Ribosomal L18p**	**x**
Nup88	**other, nuclear pore**	**x**
Ddx19	**DEAD, Superfamily II RNA helicase**	**x**

Gle1l	**other**	**x**
Nup98	**other, nuclear pore**	**x**
Lsm3	**RRM**	**x**
Sip1	**other, SIP1**	**x**
Hnrpf	**RRM**	**x**
Hnrpa0	**RRM**	**x**
Taf15	**RRM**	**x**
Dnd1	**RRM**	**x**
Sfrs12	**RRM**	**x**
Sfrs7	**RRM**	**x**
Pabpc5	**RRM**	**x**
Rbm15	**RRM**	**x**
Fubp1	**KH**	**x**
Hrb2	**KH**	**x**
Hdlbp	**KH**	**x**
Pcbp3	**KH**	**x**
Cpeb2	**RRM**	**x**
Ankhd1	**KH**	**x**
Dclre1b	**KH**	**x**
Rod1	**RRM**	**x**
Elavl1	**RRM**	**x**
Sfrs5	**RRM**	**x**
Thumpd1	**other, THUMP**	
Lrpprc	**other, PPR**	

Zfp422	**RRM**	
Fubp3	**KH**	
Pum2	**other, PUF**	
Wbscr1	**RRM**	
Etohi2	**dsRM**	
Hnrpa2b1	**RRM**	
Mki67ip	**RRM**	
Ncbp2	**RRM**	
Sfrs3	**RRM**	
Dscr1l1	**RRM**	
Eif3s4	**RRM**	
Anks1	**KH**	
Cpsf6	**RRM**	
Dgcr8	**dsRM**	
Dicer1	**dsRM**	
Matrin 3	**RRM**	
Pcbp1	**KH**	
Safb2	**RRM**	
Tnrc4	**RRM**	
Rbm25	**RRM**	
Rbm7	**RRM**	
Rbm9	**RRM**	
Pinx1	**G-patch**	**x**
Brunol6	**RRM**	**x**

Gpatc1	**G-patch**	**x**
LOC383923	**Piwi**	**x**

(‘x’ means ‘not present’.)

Supplemental Table S2: List of 199 RBPs which exist NATs in their genomic locus.

RBPs Names	Domain	NAT exists?	NAT type	NAT detail	ISH Profiled?
Pcbp4	KH	y	tail to tail	GPR62 G protein-coupled receptor 62	x
Ascc1	KH	y	head to head	AA984891	x
Boll	RRM	y	tail to tail	BC021693	x
Mint	RRM	y	head to head	AK124018	x
Elavl2	RRM	y	full length (small)	AF147374	x
Elavl4	RRM	y	full length	BE218251	x
Hnrpa1	RRM	y	full length	DB552539	x
Hnrpc	RRM	y	full length	BU607926	x
Hnrph1	RRM	y	full length	R05743	x
Hnrph2	RRM	y	full length	CA434430	x
Hnrpr	RRM	y	full length	AW136837	x
Raly	RRM	y	full length	AA074799	x
Hnrpdl	RRM	y	head to head	DA129778	x
Myef2	RRM	y	tail to tail	SLC24A5 solute carrier family 24, member 5	x
Rbm4	RRM	y	full length	BE467850	x

Msi2h	RRM	y	full length	AI694538	x
Rbms1	RRM	y	full length	AL704230	x
Cnot4	RRM	y	full length	CA439725	x
Np220	RRM	y	full length	BG207090	x
Ncl	RRM	y	full length	DB339881	x
Pabpc2	RRM	y	full length	CD364547	x
Kist	KH	y	full length	AV659210	x
Fus	RRM	y	full length	DB070270	x
Pabpn1	RRM	y	full length	BU608633	x
Sfpq	RRM	y	full length	BG028196	x
Rbm10	RRM	y	head to head	BE379249	x
Rbm3	RRM	y	head to head	AK129559	x
Rbm6	RRM	y	full length	AV759137	x
Rbmx	RRM	y	full length	AI131042	x
Rbpms	RRM	y	head to head	CF129999	x
Rnps1	RRM	y	full length	BQ672813	x
Sart3	RRM	y	full length	AI023828	x
Rbms2	RRM	y	tail to tail	AK096412	x

Rnpc1	RRM	y	head to head	AK096426	x
Sfrs10	RRM	y	full length	BU686967	x
Sfrs2	RRM	y	head to head	ET hypothetical protein ET	x
Snrpa	RRM	y	head to head	CX163256	x
Tia1	RRM	y	head to head	T55036	x
Rbm8	RRM	y	tail to tail	GNRHR2 gonadotropin-releasing hormone (type 2) receptor 2	x
Sfrs9	RRM	y	tail to tail	15E1.2 hypothetical protein LOC283459	x
Nol8	RRM	y	head to head	CENPP centromere protein P	x
Acin1	RRM	y	head to head	C14orf119 chromosome 14 open reading frame 119	x
Ppie	RRM	y	tail to tail	BMP8B bone morphogenetic protein 8b (osteogenic protein 2)	x
Adarb1	dsRM	y	head to head	AW294061	x
Prkr	dsRM	y	tail to tail	BG189068	x
Ddx9	dsRM	y	head to head	AK001442	x
Supt6h	other, S1	y	head to head	BQ310438	x

Tfip11	G-patch	y	tail to tail	CTB-1048E9.5 similar to SRR1-like protein	x
Rbm5	G-patch	y	tail to tail	AK125500	x
Hrmt1l2 (PRMT1)	other, arginine N-methyltransferase	y	head to head	IRF3 to BCL2L12	x
Eif2c3	Piwi	y	full length	AW511062	x
Peg10	Zinc Knuckle	y	full length	AW137627	x
Cnbp	other, arginine N-methyltransferase	y	head to head	DB242329	x
Zcchc7	Zinc Knuckle	y	full length	BF512512	x
Pnpt1	KH	y	full length	AW296091	x
Carm1	other, arginine N-methyltransferase	y	tail to tail	BM552692	x
Cops5	other, CSN5 domain	y	tail to tail	CSPP1 to ARFGEF1	x
Scand1	other, LR	y	head to head	DB056200	x
Ncoa6ip	other, THUMP	y	head to head	TMEM68 transmembrane protein 68	x
Ncoa3	other, PAS	y	full length	DB275059	x
Ptcd2	other, PPR	y	full length	AW087699	x
Ptcd1	other, PPR	y	tail to tail	BC001578	x
Akap1	KH	y	full length	BU675476	x
Sfrs1	RRM	y	head to head	DA002141	x

Hnrpd	RRM	y	head to head	DA129778	x
Son	dsRM	y	tail to tail	AI480262	x
Eif2c2 (AGO2)	Piwi	y	head to head	AF426412	x
Dazap1	RRM	y	full length	AK094875	x
Col4a3	RRM	y	tail to tail	AK056332	x
Hnrpl	RRM	y	full length	AA937108	x
Htf9c	RRM	y	head to head	AK097659	x
Rbmxrt	RRM	y	full length	AI131042	x
Rpo1-2	RRM	y	full length	AI223157	x
Eif3s9	RRM	y	full length	BF512712	x
Afg3l2	RRM	y	tail to tail	BC039717	x
Rbm21	RRM	y	tail to tail	AK125351	x
Poldip3	RRM	y	tail to tail	BC031838 SERHL and CTA-126B4.3	x
Rbm17	RRM	y	full length	BP398070	x
Wdr9	RRM	y	full length	AA207251	x
Slc6a8	RRM	y	head to head	BI598085	x
Hnrpa3	RRM	y	tail to tail	BI488549	x

Rbms3	RRM	y	head to head	DA506411	x
Cova1	RRM	y	full length	DB449817	x
Rnpep	RRM	y	head to head	AA150807	x
Safb	RRM	y	full length	BM563776	x
Rbm27	RRM	y	full length	AW298002	x
Tardbp	RRM	y	full length	BU675715	x
Grsf1	RRM	y	full length	BG391541	x
Rbed1	RRM	y	full length	DA107497	x
Csad	RRM	y	head to head	ZNF740 zinc finger protein 740	x
Lsm4	other, Sm protein	y	full length	AI282073	x
Lsm7	other, Sm protein	y	tail to tail	AW057599	x
Crnkl1	other, HAT	y	head to head	C20orf26 chromosome 20 open reading frame 26	x
Sf3a1	other, SWAP	y	head to head	BC018040	x
Snrpg	other, Sm protein	y	full length	EB386723	x
Cpsf5	other, mRNA cleavage factor	y	tail to tail	BF966722	x
Snrpf	other, Sm protein	y	tail to tail	DA746379	x
Prp17	other, WD40	y	full length	CA397410	x

Sf3b1	other, U2 snRNP spliceosome subunit	y	full length	CA502883	x
Prpf8	other, JAB/MPN	y	full length	AA399588	x
Nxt1	other, NTF2	y	head to head	BE891551	x
Nxf1	other, TAP-C	y	full length	DB039117	x
Rpl5	other, Ribosomal L18p	y	head to head	U66589	x
Nup88	other, nuclear pore	y	tail to tail	NM_001212	x
Ddx19	DEAD, Superfamily II RNA helicase	y	full length	BC039497	x
Gle1l	other	y	tail to tail	BG397948	x
Nup98	other, nuclear pore	y	full length	BF309280	x
Lsm3	RRM	y	full length	DB228065	x
Sip1	other, SIP1	y	full length	CA422147	x
Hnrpf	RRM	y	full length	AI133166	x
Taf15	RRM	y	full length	AK130999	x
Dnd1	RRM	y	tail to tail	WDR55 WD repeat domain 55	x
Sfrs12	RRM	y	full length	CA312467	x
Sfrs7	RRM	y	full length	DA568942	x

Pabpc5	RRM	y	full length	DA375776	x
Rbm15	RRM	y	full length	BM999102	x
Fubp1	KH	y	head to head	NEXN to C1orf118	x
Hrb2	KH	y	tail to tail	GLIPR1 GLI pathogenesis-related 1 (glioma)	x
Hdlbp	KH	y	head to head	NM_001008491 SEPT2 septin 2	x
Cpeb2	RRM	y	tail to tail	AI760149	x
Ankhd1	KH	y	full length	BI793092	x
Dclre1b	KH	y	tail to tail	AK123199	x
Rod1	RRM	y	full length	BU607910	x
Elavl1	RRM	y	full length	W37464	x
Sfrs5	RRM	y	tail to tail	T67695	x
Thumpd1	other, THUMP	y	full length	DB543799	
Lrpprc	other, PPR	y	full length	BC031947	
Zfp422	RRM	y	tail to tail	BC026193	
Fubp3	KH	y	full length	DB524448	
Pum2	other, PUF	y	full length	BF513882	
Wbscr1	RRM	y	head to head	AI863284	

Etohi2	dsRM	y	tail to tail	BG219344	
Hnrpa2b1	RRM	y	head to head	CBX3 chromobox homolog 3 (HP1 gamma homolog, Drosophila)	
Mki67ip	RRM	y	tail to tail	AK098264	
Ncbp2	RRM	y	full length	DA277609	
Sfrs3	RRM	y	full length	BX464843	
Dscr1l1	RRM	y	full length	BC043004	
Eif3s4	RRM	y	tail to tail	P2RY11 purinergic receptor P2Y, G-protein coupled, 11	
Anks1	KH	y	full length	AI243659	
Cpsf6	RRM	y	full length	AK098338	
Dgcr8	dsRM	y	full length	CA442060	
Matrin 3	RRM	y	full length	CB242024	
Safb2	RRM	y	full length	BM563776	
Tnrc4	RRM	y	full length	DB535646	
Rbm25	RRM	y	full length	CR739627	
Rbm7	RRM	y	full length	BG196362	
Rbm9	RRM	y	full length	CB267142	
Pinx1	G-patch	y	tail to tail	PINX1 PIN2-interacting protein 1 BC043573	x

Brunol6	RRM	y	tail to tail	BC034424	x
Gpatc1	G-patch	?			x
LOC383923	Piwi	?			x
Pcbp2	KH	y	tail to tail	MAP3K12 mitogen-activated protein kinase kinase kinase 12	x
Igf2bp1	KH	y	head to head	BE044435	x
Fxr1	KH	y	tail to tail	BU686455	x
Hnrpk =hnRNPK	KH	y	full length	AW978702	x
Igf2bp3	KH	y	tail to tail	AK127742	x
Khdrbs1	KH	y	full length	CA417903	x
Qk	KH	y	full length	DB530476	x
Khdrbs2	KH	y	full length	CA391235	x
Khdrbs3	KH	y	full length	CA388804	x
Brunol4	RRM	y	tail to tail	DB209115	x
Cpeb	RRM	y	head to head	BC050629	x
Cugbp1	RRM	y	tail to tail	PTPMT1 and KBTBD4	x
Cugbp2	RRM	y	full length	BM931184	x
G3bp2	RRM	y	full length	BM978447	x

Ssb	RRM	y	tail to tail	METTL5 methyltransferase like 5	x
Nsap1=hnRNP-Q	RRM	y	full length	DA447957	x
Ptbp1	RRM	y	full length	BM691399	x
U2af1-rs1	RRM	y	full length	BU619109	x
U2af1-rs2	RRM	y	full length	BC039434	x
Synj2	RRM	y	full length	BM683410	x
Tial1	RRM	y	full length	DB080956	x
Ppil4	RRM	y	full length	DB542130	x
Rbm19	RRM	y	full length	DA295001	x
Rbm22	RRM	y	full length	DB572704	x
Nono	RRM	y	full length	DA667525	x
Sfrs6	RRM	y	full length	CD243053	x
Rbm14	RRM	y	full length	BE467850	x
Pabpc1	RRM	y	full length	CD364547	x
Pspc1	RRM	y	full length	DR978109	x
Hnrpm	RRM	y	full length	BC045573	x
Rbm12	RRM	y	full length	BM968574	x
Tnrc6	RRM	y	full length	BX495114	x

Rnpc2	RRM	y	full length	BG429761	x
A2bp1	RRM	y	full length	BM669724	x
Cirbp	RRM	y	full length	BM665199	x
Stau2	dsRM	y	full length	CK818592	x
Stau1	dsRM	y	full length	CA439621	x
Prkra	dsRM	y	full length	NEB nebulin	x
Ilf3	dsRM	y	full length	DA854620	x
Adar=adar1	dsRM	y	full length	CD514840	x
Pdcd11	other, S1	y	full length	AY007124	x
Pum1	other, PUF	y	full length	DB521106	x
Hrmt1l1	other, arginine N-methyltransferase	y	full length	BQ017509	x
Piwil2	Piwi	y	full length	BQ448561	x
Eif2c4	Piwi	y	full length	BQ017637	x
Hnrpa0	RRM	y	tail to tail	NM_016603	x
Pcbp3	KH	y	head to head	DA117170	x
Dicer1	dsRM	y	full length	AA931786	
Pcbp1	KH	y	head to head	DA872092	

('y' means 'Yes' and 'x' means 'not present')

Supplemental Table S3: List of 12 NATs which had been perfectly identified by Reverse Transcription-PCR (RT-PCR).

RBPs Names	NAT exists?	NAT type and detail	NAT detail	Domain	ISH Profiled?
Pcbp2	y	tail to tail	MAP3K12 mitogen-activated protein kinase kinase kinase 12	KH	x
Hnrpk =hnRNPK	y	full length	AW978702	KH	x
Ssb	y	tail to tail	METTL5 methyltransferase like 5	RRM	x
Nsap1=hnRNP-Q	y	full length	DA447957	RRM	x
Ptbp1	y	full length	BM691399	RRM	x
Adar=adar1	y	full length	CD514840	dsRM	x
Hnrpa0	y	tail to tail	NM_016603	RRM	x
Pcbp3	y	head to head	DA117170	KH	x
Dicer1	y	full length	AA931786	dsRM	
Pcbp1	y	head to head	DA872092	KH	Present
Cirbp	y	full length	BM665199	RRM	x
Hnrpa1	y	full length	DB552539	RRM	Present

('y' means 'Yes' and 'x' means 'not present')

Supplemental Table S4: List of primers for RACE and PCR.

name	application	Sequence (5'-3')
PTB-AS-5'RACE-GSP1	RACE	GTAATTAAGTCACAGGCAGG
PTB-AS-5'RACE-GSP2	RACE	CACCACGCCTTCACCTGCAG
PTB-AS-5'RACE-GSP3	RACE	GCCTGCCTCTGATGCTGGGAC
PTB-AS-5'RACE-GSP4	RACE	CGTAAAAGCGTGTAACAAGGGTG
PTB-AS-3'RACE-GSP1	RACE	TACTGAGCCTGGAATTGC
PTB-AS-3'RACE-GSP2	RACE	CACCCTTGTTACACGCTTTTACG
PTB-AS-3'RACE-GSP3	RACE	GAGCACAAAGACAGGAGGAGCG
PTB-AS-3'RACE-GSP4	RACE	CTGCAGGTGAAGGCGTGGTG
PTB-AS-3'RACE-GSP5	RACE	CCTGCTCTCTGGAAACTGGGTC
PTB-AS-Northern-probe-F	Northern	CCCAAGCTTGCTCTTGGTCATTCGCTCTGG
PTB-AS-Northern-probe-R	Northern	CGGAATTCCTGTGTTTTGCCTGCCTCTGA
PTB-AS-biotin-probe-F	Biotin pull down	CCCAAGCTTGCTCTTGGTCATTCGCTCTGG
PTB-AS-biotin-probe-R	Biotin pull down	CGGAATTCTGTGGTATTACCTTGTATGCTGTTACT

GAPDH-F	qRT-PCR	GGTCATCCATGACAACTTTGG
GAPDH-R	qRT-PCR	GGCCATCACGCCACAG
PTB-AS-F	qRT-PCR	CAGAGGCAGGCAAAACACAG
PTB-AS-R	qRT-PCR	GACCCAGTTTCCAGAGAGCAG
PTB-F	qRT-PCR	CTGCAGCAAACGGAAATGACAG
PTB-R	qRT-PCR	GTTCATCTCGATGAAGGCCTGG
PTB-AS Reverse Transcript	qRT-PCR	GACCCAGTTTCCAGAGAGCAG
Malat1-F	qRT-PCR	CTTCCCTAGGGGATTTCAGG
Malat1-R	qRT-PCR	GCCCACAGGAACAAGTCCTA
PTB-AS-plenti6-F	overexpression	GAAGATCTGCTCTTGGTCATTCGCTCTGG
PTB-AS-plenti6-R	overexpression	CCGCTCGAGTGTGGTATTACCTTGTATGCTGTTACT
GSP-Reverse Transcript	overexpression	GTGGTATTACCTTGTATGCTG
PTB-3'UTR-luc-F	Luciferase	CCGCTCGAGctccttctccaagtccaccatc
PTB-3'UTR-luc-R	Luciferase	GCTCTAGAGAACGGAGCGAGGATACAGAAG
PTB-plenti6-F	overexpression	CGGGATCCAtggacggcattgtcccag
PTB-plenti6-R	overexpression	CCGCTCGAGCTAGATGGTGGACTTGGAGAAGG

PTB-AS-shRNA-F	Lentivirus	CCGGCAGAAAGAGGAAGCCAGCAACGAAGCTCGAGCTTCGTTGCTGGCTTCCTCTTTCTGTTTTTG
PTB-AS-shRNA-R	Lentivirus	AATTCAAAAACAGAAAGAGGAAGCCAGCAACGAAGCTCGAGCTTCGTTGCTGGCTTCCTCTTTCTG
PTB-3'UTR-RT-F	Half-life	GAAGTGACCTTAGCAGACCAGAG
PTB-3'UTR-RT-R	Half-life	CACAAGGAAGCCAAGTCGTG
PTB-3'UTR-P1	RPA	AGAAGGAGAACGCCCTAGTG
PTB-3'UTR-P2	RPA	TCTGGAAGTTCTTGGAGCCC
PTB-3'UTR-P3	RPA	CAGGCTCAGTATTGTGACCG
PTB-3'UTR-P4	RPA	AACACAGGGCTAGACAAGGG
SND1-F	qRT-PCR	GGTGCCCCAAGATGATGATG
SND1-R	qRT-PCR	GGTATTCTGTGATCACTTTCTGGA
Universe miRNAs Rltm-R	qRT-PCR	GTGCAGGGTCCGAGGT
U6-RT	qRT-PCR	GTCGTATCCAGTGCAGGGTCCGAGGTATTCGCACTGGATACGACAAAATATG
U6-F	qRT-PCR	GCGCGTCGTGAAGCGTTC
mir-9-RT	qRT-PCR	GTCGTATCCAGTGCAGGGTCCGAGGTATTCGCACTGGATACGACTCATAC
mir-9-F	qRT-PCR	CGGCCGTCTTTGGTTATCTAGC
mir-133-RT	qRT-PCR	GTCGTATCCAGTGCAGGGTCCGAGGTATTCGCACTGGATACGACCAGCTG

mir-133-F	qRT-PCR	GCGCTTTGGTCCCCTTCAAC
PTB-AS-stealth-si1	siRNA	CUUCGUUGCUGGCUUCCUCUUUCUG
PTB-AS-stealth-si2	siRNA	UGCGGGCCAGAGCGAAUGACCAAGA

Supplemental Table S5: Details of candidate proteins

Protein Symbol	Alias	Main Cell Localizations	Function	Reference(Pubmed IDs)
SND1	p100; TDRD11; Tudor-SN	extracellular, nucleus, cytosol	RNA binding nucleic acid binding transcription cofactor activity nuclease activity protein binding	22681889 7651391 20642132
hnRNP U	SAFA; HNRPU; U21.1; pp120; EIEE54; GRIP120	cytoskeleton, nucleus, extracellular	nucleotide binding RNA polymerase II core binding core promoter binding TFIIH-class transcription factor binding DNA binding	 10490622 10490622 9204873
SFPQ	PSF; POMP100; PPP1R140	nucleus, extracellular	transcription regulatory region sequence-specific DNA binding RNA polymerase II distal enhancer sequence-specific DNA binding core promoter binding nucleic acid binding DNA binding	 25765647

LGALS3BP	90K; M2BP; gp90; CyCAP; BTBD17B; MAC-2-BP; TANGO10B	extracellular, nucleus	scavenger receptor activity	
HDLBP	HBP; VGL; PRO2900	plasma membrane, cytosol, extracellular, nucleus	RNA binding protein binding lipid binding cadherin binding	22658674 24725430 1318310 25468996
PTBP1	PTB; PTB2; PTB3; PTB4; pPTB; HNRPI; PTB-1; PTB-T; HNRNPI; HNRNP-I	extracellular, nucleus	nucleic acid binding RNA binding protein binding poly-pyrimidine tract binding pre-mRNA binding	 22658674 10653975 1906036 16260624
HNRNPR	HNRPR; hnRNP-R	nucleus	nucleic acid binding RNA binding mRNA 3-UTR binding protein binding	 9421497 16169070
DHX9	LKP; RHA; DDX9; NDH2; NDHI	cytoskeleton, nucleus, cytosol	RNA polymerase II core binding core promoter binding regulatory region RNA binding RNA polymerase II transcription factor binding RNA polymerase II transcription cofactor activity	11416126 11038348 28355180 17303075 11416126

CKAP4	p63; CLIMP-63; ERGIC-63	plasma membrane, extracellular, cytoskeleton, nucleus, endoplasmic reticulum, cytosol	RNA binding	22658674
ELAVL1	HUR; Hua; MelG; ELAV1	nucleus, cytosol	nucleic acid binding RNA binding double-stranded RNA binding mRNA binding mRNA 3-UTR binding	 19561594 21266579 10660597
PABPC1	PAB1; PABP; PABP1; PABPC2; PABPL1	extracellular, nucleus, cytosol	nucleic acid binding RNA binding mRNA 3-UTR binding protein binding protein C-terminus binding	 25225333 16126846 11051545 15663938
RPL10	QM; L10; NOV; AUTSX5; DXS648; MRXS35; DXS648E	nucleus, cytosol	RNA binding structural constituent of ribosome protein binding translation regulator activity	 12962325 10508860 26290468
SLC25A6	ANT; AAC3; ANT3; ANT 2; ANT 3; ANT3Y	extracellular, mitochondrion, nucleus	ATP:ADP antiporter activity protein binding adenine transmembrane transporter activity transmembrane transporter activity	2541251 21370995
RPS2	S2; LLREP3	extracellular, nucleus, cytosol	RNA binding mRNA binding	22658674 18464793

			structural constituent of ribosome	15883184
			protein binding	15473865
			fibroblast growth factor binding	16263090
KHSRP	FBP2; KSRP; FUBP2	nucleus, cytosol	nucleic acid binding DNA binding RNA binding mRNA binding protein binding	22658674 16126846
HNRNPC	C1; C2; HNRNP; HNRPC; SNRPC	extracellular, nucleus, cytosol, cytoskeleton	RNA polymerase II proximal promoter sequence-specific DNA binding RNA polymerase II distal enhancer sequence-specific DNA binding nucleic acid binding RNA binding mRNA 3-UTR binding	16217013 16217013 9731529 16010978
RRBP1	RRp; hES; ES130; ES/130	endoplasmic reticulum	RNA binding receptor activity	22681889 9628588
HNRNPK	AUKS; CSBP; TUNP; HNRPK	extracellular, nucleus, cytoskeleton	RNA polymerase II proximal promoter sequence-specific DNA binding transcriptional activator activity, RNA polymerase II proximal promoter	20371611 20371611

			sequence-specific DNA binding nucleic acid binding DNA binding single-stranded DNA binding	20371611
HSP90B1	ECGP; GP96; TRA1; GRP94; HEL35; HEL-S-125m	extracellular, nucleus, endoplasmic reticulum, cytosol	RNA binding calcium ion binding protein binding ATP binding protein phosphatase binding	11958450 10497210 9596688 19000834
SLC3A2	4F2; CD98; MDU1; 4F2HC; 4T2HC; NACAE; CD98HC	plasma membrane, extracellular, nucleus, cytosol	RNA binding double-stranded RNA binding catalytic activity calcium:sodium antiporter activity protein binding	22658674 21266579 10673541 10506149
MYH9	MHA; FTNS; EPSTS; BDPLT6; DFNA17; NMMHCA; NMHC-II-A; NMMHC-IIA	plasma membrane, extracellular, nucleus, cytosol, cytoskeleton	microfilament motor activity nucleotide binding RNA binding motor activity actin binding	12237319 22681889 12421915 15065866
COPA	AILJK; HEP-COP	extracellular, endoplasmic reticulum, cytosol, golgi apparatus	hormone activity structural molecule activity	

RPL23	L23; rpL17	extracellular, nucleus, cytosol	transcription coactivator binding RNA binding structural constituent of ribosome protein binding ubiquitin protein ligase binding	19160485 22658674 12962325 15314173 15314173
HSPB1	CMT2F; HMN2B; HSP27; HSP28; Hsp25; SRP27; HS.76067; HEL-S-102	extracellular, nucleus, cytosol, cytoskeleton	RNA binding protein kinase C binding protein binding protein kinase C inhibitor activity protein kinase binding	22658674 11003656 8774846
YBX1	YB1; BP-8; CSDB; DBPB; YB-1; CBF-A; CSDA2; EFI-A; NSEP1; NSEP-1; MDR-NF1	extracellular, nucleus, cytosol	RNA polymerase II proximal promoter sequence-specific DNA binding transcriptional activator activity, RNA polymerase II proximal promoter sequence-specific DNA binding nucleic acid binding DNA binding chromatin binding	18809583 18809583 2977358
RPS8	S8	extracellular, nucleus, cytosol	RNA binding structural constituent of ribosome protein binding	22658674

FUBP3	FBP3	nucleus	RNA polymerase II proximal promoter sequence-specific DNA binding transcriptional activator activity, RNA polymerase II proximal promoter sequence-specific DNA binding nucleic acid binding DNA binding RNA binding	8940189 8940189 22658674
HADHA	GBP; ECHA; HADH; LCEH; MTPA; LCHAD; TP-ALPHA	extracellular, mitochondrion	fatty-acyl-CoA binding catalytic activity 3-hydroxyacyl-CoA dehydrogenase activity acetyl-CoA C-acetyltransferase activity acetyl-CoA C-acyltransferase activity	8135828 8135828
EIF2AK2	PKR; PRKR; EIF2AK1; PPP1R83	nucleus, cytosol	RNA binding double-stranded RNA binding protein kinase activity protein serine/threonine kinase activity eukaryotic translation initiation factor 2alpha kinase activity	22681889 21266579 21123651 1695551 25329545
RPS16	S16	extracellular, nucleus, cytosol	RNA binding	17881366

			structural constituent of ribosome	
			protein binding	24725412
CCT3	CCTG; PIG48; TRIC5; CCT-gamma; TCP-1-gamma	extracellular, nucleus, cytosol, plasma membrane	RNA binding	22681889
			protein binding	12620389
			ATP binding	
			protein binding involved in protein folding	
			unfolded protein binding	
IGF2BP3	KOC; CT98; IMP3; KOC1; IMP-3; VICKZ3	nucleus, cytosol	RNA binding	22658674
			mRNA 3-UTR binding	20080952
			protein binding	17289661
			translation regulator activity	9891060
			mRNA 5-UTR binding	9891060
MTDH	3D3; AEG1; AEG-1; LYRIC; LYRIC/3D3	plasma membrane, nucleus, endoplasmic reticulum	RNA polymerase II transcription factor binding	18316612
			transcription coactivator activity	18316612
			RNA binding	22658674
			double-stranded RNA binding	21266579
			protein binding	18316612
RPN1	HRD2; NAS1	extracellular, endoplasmic reticulum, cytosol	RNA binding	22658674
			contributes_to dolichyl-diphosphooligosaccharide-protein glycotransferase activity	15835887
			protein binding	22988243

			transferase activity	
			transferase activity, transferring glycosyl groups	
HNRNPL	HNRPL; hnRNP-L; P/OKcl.14	extracellular, nucleus	nucleic acid binding	
			RNA binding	22658674
			protein binding	11809897
			transcription regulatory region DNA binding	11809897
			pre-mRNA intronic binding	25623890
GLUD1	GDH; GDH1; GLUD	mitochondrion	glutamate dehydrogenase (NAD+) activity	11903050
			glutamate dehydrogenase [NAD(P)+] activity	11032875
			protein binding	16959573
			ATP binding	
			GTP binding	11032875
FUBP1	FBP; FUBP; hDHV	nucleus	DNA binding	
			single-stranded DNA binding	8125259
			DNA binding transcription factor activity	8125259
			RNA binding	22658674
			protein binding	21285945
ACLY	ACL; ATPCL; CLATP	extracellular, nucleus, cytosol, plasma membrane	catalytic activity	
			ATP citrate synthase activity	23932781
			protein binding	23932781
			ATP binding	1371749

			transferase activity	
PRKDC	HYRC; p350; DNAPK; DNPK1; HYRC1; IMD26; XRCC7; DNA-PKcs	nucleus, cytosol, extracellular	DNA binding double-stranded DNA binding RNA binding protein kinase activity protein serine/threonine kinase activity	22504299 22658674 22504299
RPS18	KE3; S18; HKE3; KE-3; D6S218E	nucleus, cytosol, extracellular	nucleic acid binding RNA binding structural constituent of ribosome protein binding rRNA binding	22658674 22720776
UQCRC2	QCR2; UQCR2; MC3DN5	extracellular, nucleus, mitochondrion	metalloendopeptidase activity protein binding zinc ion binding protein complex binding metal ion binding	21078624
KRT2	K2e; KRTE; CK-2e; KRT2A; KRT2E	nucleus, cytosol, extracellular, cytoskeleton	structural molecule activity structural constituent of cytoskeleton protein binding cytoskeletal protein binding structural constituent of epidermis	1380918 25416956 7543090
PABPC4		nucleus, cytosol	RNA binding	22658674

	mRNA binding	
APP1; APP-1;	protein binding	11369516
PABP4; iPABP	poly(A) binding	8524242
	poly(U) RNA binding	8524242